AD-A137 421 TROPICAL WEATHER SYSTEM AND OCEAN MODELING(U) SCIENCE APPLICATIONS INC MCLEAN VA S CHANG 1983 SAI-83-1155 N00014-82-C-2306 1/2

UNCLASSIFIED F/G 4/2 NL

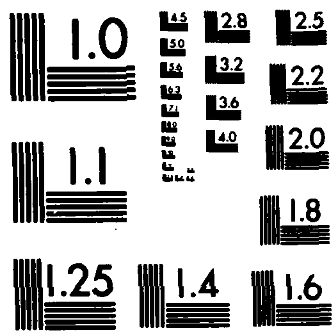

MICROCOPY RESOLUTION TEST CHART
NATIONAL BUREAU OF STANDARDS-1963-A

(12)

AD A137421

TROPICAL WEATHER SYSTEM

AND OCEAN MODELING

FINAL REPORT 83-1155

Contract N00014-82-C-2306

DTIC
ELECTE
FEB 1 1984

S A

DTIC FILE COPY

SCIENCE APPLICATIONS, INC.

83 [illegible] 014

TROPICAL WEATHER SYSTEM

AND OCEAN MODELING

FINAL REPORT 83-1155

SCIENCE APPLICATIONS, INC.

Post Office Box 1303, 1710 Goodridge Drive, McLean, Virginia 22102, (703) 821-4300

TROPICAL WEATHER SYSTEM AND OCEAN MODELING

FINAL REPORT SAI 83-1155

Submitted to

Atmospheric Physics Branch
Space Science Division
Naval Research Laboratory
Washington, D.C. 20375

Prepared Under:

Contract No. N00014-82-C-2306

Prepared by:

Simon Chang
Science Applications, Inc.
McLean, Virginia 22012

SCIENCE APPLICATIONS, INCORPORATED

1710 Goodridge Drive, McLean, Virginia 22102 (703)734-5840

This final technical report documents the research efforts in the numerical simulations of tropical weather systems carried out under the auspices of ONR Contract N00014-82-C-2306, for the Atmospheric Physics Branch, Space Science Division, of the Naval Research Laboratory (NRL).

Our research efforts mainly concentrate in two major study areas: the interactions between two tropical cyclones and the construction of an axisymmetric ocean model. The research in both of these areas has been completed and reported in two articles. A paper entitled "A Numerical Study of the Interactions Between Two Tropical Cyclones" was accepted by the Monthly Weather Review and is to be published in the 1983 September issue. The draft of a second article on the ocean model has been completed. Both articles are included as Appendices in this final report. We have also attached a listing of the computer code of the ocean model, which is also stored in and accessible from the TI-ASC of NRL. Here, a brief summary of the study result will be given.

The interactions between atmospheric vortex pairs are simulated and studied with a nondivergent barotropic model and a three-dimensional tropical cyclone model (NRL/SAI mesoscale model). Numerical experiments with nondivergent barotropic vortex pairs show that the relative movements of the vortices are sensitive to the separation distance

Letter on file

A-1

and the characteristics of the swirling wind of the vortex. No observed mutual attraction is found in any of the nondivergent, barotropic vortex pairs tested.

Results from the 3D NRL/SAI tropical cyclone model show that on a constant-f plane with no mean wind, the movements of the two interacting tropical cyclones consist of a mutual cyclonic rotation, attraction, and eventual merging, in agreement with Fujiwhara's description. The displacement of one interacting storm in the mutual rotation is proportional to the combined strength of the binary system, but inversly proportional to the size of the storm and to the square of the separation distance. The rate of merging is related to the development of a mean secondary circulation on the radial-vertical plane, and is quite independent of the strength of the two tropical cyclones.

The latitudinal variation of the Coroilis parameter adds a northwest beta drift to the trajectories. Depending on their relative strength and location, the beta drift can either speed up the merging process or separate the two interacting tropical cyclones.

The axisymmetric ocean model consists of primitive equations for the conservation of momenta in three spatial dimensions and the buoyancy. A Boussineq assumption is made so that the background stratification is kept constant, the horizontal and vertical diffusion is of the Fickian type.

A leapfrog temporal integration is employed. The grid is fully staggered as Arakawa C type. The system is non-hydrostatic, the resultant elliptic equation for the pressure is solved by a stablized error vector propagation technique. The basic equations, the finite differencing form, and boundary conditions are discussed in detail in the attached Appendix.

APPENDIX I

A NUMERICAL STUDY OF THE INTERACTIONS BETWEEN TWO TROPICAL CYCLONES

A Numerical Study of the Interactions Between Two Tropical Cyclones

Simon Wei-Jen Chang

Science Applications, Inc.

McLean, VA 22102

June 1983

ABSTRACT

The interactions between atmospheric vortex pairs are simulated and studied with a nondivergent barotropic model and a three-dimensional tropical cyclone model.

Numerical experiments with nondivergent barotropic vortex pairs show that the relative movements of the vortices are sensitive to the separation distance and the characteristics of the swirling wind of the vortex. No mutual attraction is found in any of the nondivergent, barotropic vortex pairs tested.

Results from the 3D tropical cyclone model show that on a constant-f plane with no mean wind, the movements of the two interacting tropical cyclones consist of a mutual cyclonic rotation, attraction, and eventual merging, in agreement with Fujiwhara's description. The displacement of one interacting storm in the mutual rotation is proportional to the combined strength of the binary system, but inversly proportional to the size of the storm and to the square of the separation distance. The rate of merging is related to the development of a mean secondary circulation on the radial-vertical plane, and is quite independent of the strength of the two tropical cyclones.

The latitudinal variation of the Coriolis parameter adds a northwest beta drift to the trajectories. Depending on their relative strength and location, the beta drift either speeds up the merging process or separates the two interacting tropical cyclones.

1. INTRODUCTION

When two tropical cyclones are present simultaneously in the same region, it is often observed that they rotate around each other with decreasing separation between them in the absence of large scale wind flow (Fig. 1). The phenomenon was made well-known by Fujiwhara (1921), and is therefore referred to as the Fujiwhara effect. By laboratory experiment and geophysical observation, Fujiwhara (1923, 1931) demonstrated that the relative motion of two counterclockwise vortices was a counterclockwise rotation. Haurwitz (1951) examined several tropical cyclone pairs by introducing the concept of center of mass around which the two tropical cyclones rotate about each other. By approximating the circulation around a tropical cyclone with that of a Rankine vortex, Haurwitz (1951) derived a relationship between the rotation rate and the sum of the total mass circulation of the two tropical cyclones. Many discrepancies were found when he applied the relationship to observations. Haurwitz attributed the discrepancies to the influence of large scale flow and lack of data, which led to deficiency in analyses.

Hoover (1961) studied binary tropical cyclones in both the Atlantic and Western Pacific Oceans. He found that the interaction between tropical cyclone pairs in the Western Pacific Ocean agrees with Fujiwhara's description while those pairs in the Atlantic Ocean rotated in an anticyclonic sense. He suggested that the different large scale atmospheric flow patterns in the two basins may have caused the binary systems to behave differently. The influence of the large scale flow was also noted by Liu and Wang (1966). They found that two interacting tropical cyclones in the Western Pacific are not always attracted to each other when there are strong shears in the environmental flow. Recently, Dong and Neumann (1982)[1] found that storm pairs exhibiting behavior most in accordance with Fujiwhara's description were located in the Intertropical Convergence Zone where horizontal shears in large scale flow are negligible. They suggest that the effects of environmental flows be filtered before the real Fujiwhara effects can be determined. But to define and remove the large scale flows from observational data is difficult to accomplish.

Over the 35 year period 1946-1981, storm pairs known to have interactions averaged 1.5 annually in Western North Pacific and 0.33 annually in the Atlantic (Dong and Neumann, 1982). The presence of binary interacting has been noted to have contributed to forecast errors of tropical cyclone tracks (Brand, 1970; Jarrell _et_. _al_.; 1978; Neumann, 1982). Forecasting as well as analyzing a single tropical cyclone is often hindered by the paucity of observational data in the tropical cyclone basin (Neumann, 1982); the presence of two storms in close proximity can further compound the difficulties.

The purpose of our study is to investigate the interactions between two tropical cyclones by numerical simulations. Because the spatial resolutions of the models are better than the current observational network, and because numerical models can be controlled to produce "clean" results void of undesirable factors, analyzing realistic numerical simulations can sometimes result in a better isolation and understanding of the phenomenon than can be acheived from an observational approach. In this paper we will first determine the role of vorticity advection between the two vortices. For this purpose, a nondivergent, barotropic model is introduced to test two types of vortex pairs with different

---

[1]Dong, K. and C. J. Neumann, 1982: On the relative motion of binary tropical cyclones. Regional Scientific Conference on Tropical Meteorology, Tsukuba Ibaraki, Japan, Oct. 1982.

swirling winds. These barotropic tests will be presented in Section 2. In Section 3, three-dimensional simulations of the interactions between two diabatically driven tropical cyclones on a constant-f plane and with variable f will be discussed. Our findings will be summarized in Section 4.

2. INTERACTIONS BETWEEN NONDIVERGENT, BAROTROPIC VORTEX PAIRS

In this section, we investigate the interactions between nondivergent barotropic vortex pairs. Through the interactions of such vortex pairs, we can determine the contribution of horizontal advection of vorticity, because in such a system advection is the only mechanism for interaction. A description of the nondivergent, barotropic model will be presented first, and the experimental design and the results will then be discussed.

a. Nondivergent Barotropic Model

The simple non-divergent, barotropic model can be described as

$$\frac{\partial}{\partial t} \nabla^2 \psi = -\underset{\sim}{V}_\psi \cdot (\nabla^2 \psi + f), \text{ and} \tag{1}$$

$$\underset{\sim}{V}_\psi = \hat{k} \times \underset{\sim}{\nabla}\psi \tag{2}$$

where f is the Coriolis parameter, ψ is the stream function, $\underset{\sim}{V}\psi$ is the nondivergent wind, and $\hat{k}$ is a vertically pointing unit vector. The boundary conditions for (1) and (2) are Neumann, i.e., $\nabla^2 \Psi = 0$ at boundaries. The model has 51 x 51 grid points with a uniform horizontal resolution of 50 km. The relevant elliptic equation

$$\nabla^2 \psi = \zeta \tag{3}$$

where the relative vorticity is defined by

$$\zeta = \hat{k} \cdot \underset{\sim}{\nabla} \times \underset{\sim}{V}\psi, \tag{4}$$

is solved by a stabilized error vector propagation method (Madala, 1978).

b. Experimental Design

The major application of the nondivergent barotropic model is to determine the effects of separation distance and the radial distribution of tangential winds on the interaction of the two vortices. Two kinds of wind distributions were tested. The first kind (type A) of vortex is defined by its cyclonic swirl wind v_o as function of radius r from the vortex center

$$v_o = \begin{cases} Ar\,(1 - \sin \frac{\pi r}{r_o}), & 0 \leq r \leq r_o \\ 0, & \text{otherwise} \end{cases} \tag{5}$$

where constant $A = 4 \times 10^{-4}\ s^{-1}$ and $r_o = 400$ km. Equation (5) yields a maximum swirl of $\sim 26\ m\ s^{-1}$ at $r = 150$ km and a maximum vorticity $\zeta \cong 7.2 \times 10^{-4}\ s^{-1}$ at $r = 0$. We note that there is a cutoff of v_o at r_o.

The second kind of vortex (type B) is defined as

$$v_o = Br \exp\,(-\frac{r^2}{r_e^2}) \tag{6}$$

where the e-folding distance r_e is 150 km. By letting the constant $B = 3.6 \times 10^{-4}\ s^{-1}$, (6) yields a vortex with similar strength as that described by (5) with maximum swirl of $\sim 29\ m\ s^{-1}$ and a maximum $\zeta \cong 7 \times 10^{-4}\ s^{-1}$. Type B vortex differs from Type A in that there is no cutoff of swirl. Fig. 2 compares the radial distributions of relative vorticities described by (5) and (6).

Four initial separation distances (300, 400, 600, and 1000 km) have been tested for each type of vortex pairs. All intergrations with the barotropic model are performed with constant $f = 4.37 \times 10^{-5}\ s^{-1}$.

c. Results

Fig. 3 shows the trajectories of storm pairs having two types of swirl wind at four separation distances. It is very clear from Fig. 3 that the smaller the separation distance the faster the mutual transport. For instance, at a separation distance of 1000 km, neither type A vortex pair (with swirl cutoff at r = 300 km) nor type B vortex pair can induce mutual motion. But at a separation distance of 400 km, they move at a speed of $\sim$400 km day^{-1}.

It is also evident that the mutually-induced motions of type A and type B vortices are very different, in spite of the values of constants for A and B which were chosen to give vortices of similar strength. Furthermore, the trajectories of type A vortex pairs are more anticyclonic. This may be a result of the fact that type B vortices have positive vorticities at $r \leq$ 200 km whereas the vorticities of type A vortices change sign at r = 150 km (Fig. 2). Only vortex pairs at small separation distances rotate in a cyclonic fashion because they interact with positive shears. The motion of vortices in our model can only be caused by the advection of vorticity, the shear in one vortex can very much determine the movement of the other. These results indicate that the mutual motion of two interacting nondivergent, barotropic vortex pair are quite sensitive to the charateristics of the swirl winds.

In all the experiments illustrated in Fig. 3 the storm pairs drift apart, there is no mutual attraction as observed in some interacting typhoons. This suggests that the observed mutual attraction in typhoon pairs may be due to the divergence and/or convergence that is not included in the barotropic model. Indeed, complicated diabatic processes in tropical cyclone such as long wave radiation, surface boundary layer effects and moist convection generate convergent flow in lower troposphere and divergent flow in upper troposphere. The irrotational component of the vortex circulation may be responsible for the occurrence of the observed cyclonic rotation and mutual attraction.

3. INTERACTIONS BETWEEN TROPICAL CYCLONE PAIRS

We have seen that nondivergent pairs do not cause a mutual motion similar to the description of Fujiwhara. The observed Fujiwhara effects may be due to dynamics that can only be resolved by a more complete model. To see that, we will simulate the interactions between two diabatically driven tropical cyclones with a three-dimensional model.

a. Three-dimensional Tropical Cyclone Model

The baroclinic model is identical to the one in Chang and Madala (1980) and Chang (1982), except for parameterization of the latent heating. The governing equations are in surface-pressure-weighted flux form for conservation of momentum, temperature and water vapor. The normalized pressure $\sigma = p/p_s$ is the vertical coordinate, where p_s is the surface pressure. The system is assumed hydrostatic. The bulk boundary layer parameterization is based on a generalized similarity theory (Chang, 1981). The model has 51 x 51 horizontal grid points with seven sigma layers in the vertical. The horizontal resolution if $\frac{1}{2}^{\circ}$ in both the latitudinal and longtitudinal directions. The east-west boundaries are cyclic. The boundary conditions at the north and south boundaries are such that the second derivatives of thermodynamic variables normal to the boundaries vanish. In addition, diffusion coefficients are increased near the north and south boundaries to damp numerical noise there.

Kuo's parameterization was used in Chang and Madala (1980) and Chang (1982), but a prescribed heating is applied in this model as done by Anthes (1971) in a axisymmetric model. The heating rate here is defined as

$$\dot{Q}(r,\sigma) = \begin{cases} \dot{Q}_o \cos(\frac{\pi r}{2R}) \sin[\pi(\sigma-0,1)], \text{ for } r \leq R,\ 0.1 \leq \sigma \leq 0.9 \\ 0, \text{ otherwise} \end{cases} \tag{7}$$

where r is the distance between a grid point and the low pressure center, and R = 300 km is the limit of the heating function. Two values of $\dot{Q}_o$, 100 K day^{-1} and 200 K day^{-1}, have been used in various numerical experiments to define the weak and strong tropical cyclones, respectively. The vertical and horizontal distributions of the heating pattern described in (7) are illustrated in Figs. 4 and 5. The vertical heating distribution is similar to that of the differences between temperatures in convective clouds (T_c) and the environment (T) in a mean hurricane season sounding for the Gulf of Mexico as computed by a one-dimensional cloud model (Anthes, 1977, Fig 4a). The horizontal heating distribution agrees with the mean rainfall rate inferred from satellite observation in a typhoon (Adler and Rogers, 1977), except for the observed smooth fall-off at $r \geq 300$ km. No effort is attempted to simulate the eye because of the model horizontal resolution.

The heating prescribed by (7) nevertheless generates realistic circulations for tropical cyclones. Figure 6 shows the radial distribution of the quasi-steady wind speeds at the sixth ($\bar{\sigma}$ = 0.85) and seventh ($\bar{\sigma}$ = 0.965) model layers after 24 h of heating with $\dot{Q}_o$ = 200 K day^{-1}. The wind speeds have a peak at r = 1^o and decrease gradually outward without discontinuity at $r = R = 300$ km.

We note however that by using the prescribed heating in (7) the effects of the interaction between the two cyclones on the scale of the cumulus convection cannot be adequately simulated. In reality the momentum field in each storm, which affects the cumulus convection, can be modified by the proximity of another storm. A change in the cumulus convection in each storm may alter the storm's intensities, which can in turn affect the interaction between the two tropical cyclones. But these feedbacks may be secondary and are only important when the separation of the two storms is small. As a preliminary study, the more economical, prescribed heating is used to investigate the first order effects in the interaction.

b. Experimental Design

The tropical cyclone pairs in all numerical experiments (Table 1) with the 3D model are dynamically initialized by a 24h stationary heating at two locations, i.e., by applying (7) at two fixed grid points for 24h. Dong and Neumann (1982) found that in real cases when the separation distances are less than 11 degree of latitude, cyclonic rotation predominates. Therefore, the two fixed grid points for the stationary heating are set ten degree longitude apart in all experiments to ensure the occurrence of interaction. After the dynamic initialization period, the heating patterns are allowed to follow the low pressure centers. In Exps. 1-3 we simulate the Fujiwhara effects in zero large scale winds on a constant-f plane for strong-strong (Exp. 1) weak-weak (Exp. 2) and strong-weak (Exp. 3) storm pairs. Exp. 1 and 3 are repeated in Exp. 5 and 6 on a real variation of f. There is only one single tropical cyclone in Exp. 4 to help isolate the effect of the beta-drift. Unlike on a

Table 1: List of three-dimensional Numerical Experiments

Exp.	$\dot{Q}$ (K day^{-1}) Storm A	Storm B	$f(s^{-1})$	Characteristic
1	200	200	4.37×10^{-5}	strong-strong interaction
2	100	100	"	weak-weak interaction
3	100	100	"	weak-strong interaction
4	200	-	variable f	beta drift
5	200	200	"	strong-strong interaction
6	100	200	"	weak-strong interaction
7	200	100	"	strong-weak interaction

constant-f plane where geophysical orientation is not meaningful, the interactions with real f for a weak (west)-strong (east) pair and strong (west)-weak (east) pair are quite different, as we shall see later, thus Exp. 7 is conducted to study the latter situation.

c. Results on a Constant-f Plane

Fig. 7 shows the surface pressure field at 24, 48, 72, and 96h for Exp. 1. The southward displacement of storm A (west) and the northward displacement of storm B (east) at 24h indicate that their interaction has already caused the two storms to begin to rotate cyclonically in spite of the stationary heating. The merging of the two storms progresses with the merging of the outer isobars as observed (Fig. 1). By 96h, only the 996 mb isobars show two separate low pressure centers. The pressure at the center point of the model decreases by 10 mb while the approaching of the two initial low pressure centers between 24-96h can only account for a pressure decrease of 2 mb. This indicates that the mutual rotation and merging involve dynamics more complicated than merely advective processes.

Exp. 1-3 are integrated with a constant f. Therefore the orientation has little meaning and the results are independent of the absolute initial positions of the storms. Fig. 8 shows the trajectories of the storm centers in Exp. 1, in which two strong model tropical cyclones are of the same strength. The trajectories show that the two storms rotate about each other in a cyclonic fashion before the coalescence at 102h. The two trajectories are symmetric about the center of mass, which coincides with the center of the model domain. Superimposed on the symmetric rotation is a convergence of the two tropical cyclones. The distance between the two storms decreases from ∿1024 km at 24h to ∿612 km at 96h. The symmetry remains until 102h when the two heating patterns overlap and one single large area of low pressure is formed.

Exp. 2 is identical to Exp. 1 except that the heating rate is reduced by one half. The cyclonic trajectories (Fig. 9) are still remarkably symmetric about the center of mass. Because of the weaker heating, two identificable centers still exist at 120h when they are only ∿100 km apart. We note again that at small separation distances feedbacks between cumulus convection and the strom pair's interaction have been masked by the prescribed heating in our model.

The speeds at which the two tropical cyclones in Exp. 1 and 2 rotate around and approach each other are shown in Fig. 10. The tangential velocity of the cyclonic rotation in Exp. 1 increases from ∿3 m s^{-1} at 24-36h to well over 6 m s^{-1} after 72h as the separation between the two tropical cyclones becomes small. The rotation speeds in Exp. 2 are about 1 m s^{-1} slower than those in Exp. 1. However, the rate of convergence seems quite independent of the combined strength as indicated by the radial velocities in Fig. 10. The faster rotations between stronger pairs are evident observationally at small separation distances (Dong and Neumann, 1982). At larger separation distances, this relationship is not clear because the observational data contains environmental influences.

Fig. 11 shows the trajectories of the two storm center in Exp. 3, in which the maximum heating rate is storm A is only half that of storm B. We see that the two storms still rotate about each other cyclonically and that they still move toward each other. However, the trajectories are asymmetric and the weaker storm A moves much faster than the stronger storm B in a way similar to that of a binary celestial system in which the two bodies have different masses. The "mass" of a vortex is perhaps best expressed as the product of its mean angular velocity and the square of an effective radius $\bar{\omega}R^2$. We will discuss this further later. This type of interaction between storms of different intensities has been observed between Typhoons Flossie and Grace in 1950 (Liu and Wang, 1966). Instead of being stationary, the center of rotation moved within a small area defined by the lines connecting the two storm centers at different times as in Fig. 10.

Results in Exps. 1-3 demonstrate that on an f-plane with no large scale wind, interactions between two tropical cyclones cause the two storms to rotate cyclonically, to attract each other and to coalesce eventually.

In order to examine the momentum fields associated with the interaction we transform the model 500 mb wind fields in Exp. 1 onto a polar grid with respect to the center of the model domain. We now define the azimuthal mean velocity as

$$\bar{\underset{\sim}{V}} = (\bar{v}_r, \bar{v}_\theta, \bar{v}_z) = \frac{1}{2\pi}\int_0^{2\pi} (v_r, v_\theta, v_z)\, d\theta \tag{8}$$

where v_r, v_θ, v_z are radial, tangential and vertical velocities on the polar grid, and θ is the azimuthal angle. Fig. 12 shows the mean vertical (upper), tangential (middle), and radial (lower) velocities for Exp. 1 at 24, 48, 72, and 96h. It is interesting that the mean momentum fields relative to the center of domain shown here are similar to those in weak but intensifying tropical disturbances (Hawkins and Rubsam, 1968). For example, at 24h there is a maximum mean tangential velocity of ~ 4 m s^{-1} at r ~ 600 km and a minimum of ~ -2 m s^{-1} at r ~ 400 km, reflecting the cyclonic wind fields about the two storm centers. The maximum tangential velocity gradually increases to ~ 16 m s^{-1} and moves toward the center to a radius ~ 350 km at 96h. The maximum inflow also develops from 2 m s^{-1} at r ∿600 km at 24h to ∿4 m s^{-1} at r ∿350 km at 96h. The evolution of the mean vertical velocity includes the increasing magnitude and contracting radii of maximum upward motion. The development of the mean circulation is accompanied with the pressure decrease of 10 mb at the domain midpoint from 24-96h, as discussed before.

The development of the azimuthal mean circulation can also be illustrated by comparing the kinetic energy (KE) of the mean velocity (KEM) and the KE of the eddy velocity (KEE), where

$$KEM = \iint_0^{1000\ km} \tfrac{1}{2} (\bar{v}_r, \bar{v}_\theta) \cdot (\bar{v}_r, \bar{v}_\theta)\ r dr d\theta \tag{9}$$

$$KEE = \iint_0^{1000\ km} \tfrac{1}{2} (v_r', v_\theta') \cdot (v_r', v_\theta')\ r dr d\theta \tag{10}$$

$$\text{and } (v_r', v_\theta') = (v_r, v_\theta) - (\bar{v}_r, \bar{v}_\theta) \tag{11}$$

As shown by Fig. 13, the KEE, which can mostly be attributed to the circulations around the two centers, reaches a quasi-steady state after 36h. Meanwhile the KEM, representing the strength of the mean circulation as depicted in Fig. 10 around the center of rotation, steadily increases until the coalescence of the two tropical cyclones. The ratio KEE/KEM decreases from ∿3 at 24h to less than 1 at 96h.

These analyses suggest that a mean circulation relative to the center of rotation develops due to the interaction of two tropical cyclones. This mean circulation includes tangential, radial and vertical components resembling those associated with tropical cyclones. It is therefore not surprising that the trajectories of the two interacting storms are similar to the trajectories in the hurricane boundary layer (e.g. Anthes 1982, Fig. 4.6). Compared with the nondivergent, barotropic experiments in Section 2, it seems that the diabatic heating in two storms plays a cruical role for the merging of the two storms.

In additional numerical experiments, the surface friction was suppressed to test the frictional effects in the interaction. Results from these experiments were nearly identical to those presented for Exps. 1-3. We also halved the coefficients for the internal dissipation. For the same given heating rates, the interactions are nearly the same except for faster rotation rates, because the model cyclones were stronger with less internal friction. Therefore, neither surface nor internal friction seem to be critical processes in the interactions.

d. Relation of Mutual Rotation Rate to Bulk Parameters of the System

The results presented so far indicate generally that the rate of the mutual cyclonic rotation depends on the strength of the binary system and the separation distance of the two interacting storms. Perhaps by relating some extent parameters through laws governing solid body rotation, a simple description of the numerical results is attainable.

We now consider the rotation of the binary storms is similar to that of a dumbbell. The equation of motion for rotation states that the torque τ acting on the binary system is equal to the product of the rotational inertia of the system I and the angular acceleration $\dot{\omega}$ with respect to the axis of rotation, i.e.

$$\tau = I\dot{\omega} \qquad (12)$$

If we let R be an effective radius of the storm and H be the scale height, the mass of one storm can be approximated by $\rho_0 \pi R^2 H$. Because the radius of the mutual rotation is about L/2, the rotational inertia

$$I \propto \rho_0 \, (\bar{R}_A^2 + \bar{R}_B^2) H L^2 \tag{13}$$

where ρ_0 is a reference density and subscript A and B are pertinent for storms A and B, respectively.

The torque is equal to the cross product of a force and radius of rotation. The force involved in the interaction can be approximated by the advection, then it can be scaled by $\rho_0 \, \bar{V}^2/L$, where $\bar{V}$ is the velocity of the mean circulation defined by (8). Because the mean circulation depends on the combined strength of the two interacting cyclones, therefore $\bar{V} \propto \bar{v}_A + \bar{v}_B$, where $\bar{v}_A$ and $\bar{v}_B$ are the mean wind speed within the effective radius $\bar{R}_A$ and $\bar{R}_B$, respectively. Thus, the torque is proportional to

$$\tau \propto LH \, \rho_0 \, (\bar{R}_A^2 + \bar{R}_B^2) \, (\bar{v}_A + \bar{v}_B)^2 \, L^{-1} \tag{14}$$

We note that the torque contains the dimension of the kinetic energy of the two storms, which is ultimately related to the applied heating $\dot{Q}$ in our model. Substituting (13) and (14) into (12) and dropping the over-bars, we get

$$(v_A + v_B)^2 \propto \dot{\omega} L^2 \sim f\omega L^2 \tag{15}$$

In above, f^{-1} is selected as the time scale, so that $\dot{\omega} \sim \omega/T \sim f\omega$. For our purposes of examining numerical results of a limited domain model away from the equator where f remain nearly a constant, the selection of f^{-1} as a time scale is justifiable.

$$\omega \propto \frac{(v_A + v_B)}{fL^2} \qquad (16)$$

Relationship (16) states simply that the rate of the mutual rotation is proportional to the combined kinetic energy of the two interacting tropical cyclone and inversly proportional to the square of the separation distance. In addition, the displacement of one storm should be inversely proportional to its size, because the radius of rotation is inversely proportional to the mass $\pi\rho_0 R^2 H$.

In applying (16) to the numerical results, the mean wind speed within the radius of the gale force wind (17 m s^{-1}) is used as v_A and v_B. Excluding data when the separation distance is smaller than the sum of two radii of the gale force, rotation rates of binary system at every 6h were compared with $(v_A + v_B)^2/fL^2$ for Exps 1,2 and 3 (Fig. 14). It is clear the (16) is a good description of the results Exp. 1-3. The rotation rates ω and quantities $(v_A + v_B)^2/fL^2$ have a correlation coefficient of 0.81. Therefore, our numerical results can to some extent be represented by surprisingly simple relationship (16).

It should be noted, however, that (16) is arrived through several simplifying assumptions. These include approximating the mutual rotation of two vortex in the atmosphere by using solid body mechanics and excluding the merging from consideration. While (16) yields good correlation, it is only an approximation of the rotation component of the interaction.

e. The Effects of Variation of the Coriolis Parameter

Exps. 4-7 were carried out with variable Coriolis parameter, which can produce northwestward drifts of tropical cyclones in the northern hemisphere (Adem, 1956; Anthes and Hoke, 1975; Madala and Piacsek, 1975). The velocity of the drift depends on the latitude and the cyclone's circulation. To examine the free drift of a single tropical cyclone in our model, we carried out Exp. 4. As shown by trajectory C in Fig. 15, the model tropical cyclone has an initial northward movement, but changes toward the northwest after 36h, similar to the results of Anthes and Hoke (1975). The 0-72h mean drift velocity is 1.18 m s^{-1}

toward the west and 1.37 m s^{-1} toward the north. The center at 72h is $\sim 6^{o}$ to the west and $\sim 6.5^{o}$ to the north of the initial position.

The latitudinal variation of the Coriolis parameter has a pronounced effect on the trajectories of the two interacting tropical cyclones. The trajectories of the two tropical cyclones with equal strength in Exp. 5 are shown in Fig. 15. The two storms merge much faster than Exp. 1 due to the faster northwest drift of the storm located to the south. At 87h only one large low pressure center is identifiable, while in Exp. 1, two low pressure centers still existed at 96h (Fig. 7). Instead of rotating around the + point in Fig. 8 as in Exp. 1, storm A moves toward the southeast then quickly turns toward the northeast, while storm B rapidly moves northwestward and rotates cyclonically with respect to storm A. The two storms eventually merge into one at 87h, with storm B having traveled a much larger distance from its initial position than storm A. The relative trajectories of A and B with respect to trajectory C (Exp. 4) are computed. The resultant relative trajectories (not shown) are nearly the same as those in Exp. 1 (Fig. 3), indicating that the trajectories A and B in Fig. 15 is nearly a linear combination of the trajectories in Fig. 3 and the beta drift.

Exp. 6 is to be compared with Exp. 3, where storm A is weaker than storm B. The trajectories of the storm centers in Exp. 6 (Fig. 16) again appear very different from those in Exp. 3. The stronger storm B shows more noticeable northwest drift than in Exp. 3. The weaker storm A rotates cyclonically toward the southeast at a much reduced rate and with a smaller radius, apprently due to the counteracting beta drift.

Most interesting is Exp. 7, in which storm A is stronger than storm B. From 24 to 72h, the weaker storm B moves cyclonically relative to storm A.

In the meantime storm A moves slowly toward the southwest nearly perpendicular to and away from storm B. The trajectories take a strange turn after 72h because the two storms now are close to the boundaries and start to influence each other through the east-west boundaries because of the cyclic boundary conditions there.

The distictively different behavior between Exps. 5-7 can be explained by examining schematically the vectors of forces upon each storm. We let the northwest drift be proportional to the storm's intensity and size (Rossby, 1948; Adem, 1956) and the force due to the interaction be proportional to the combined strength of the binary system but inversely proportional to the strength of individual storm as discussed in Section 3c. Figure 17 shows the vectors and the resultant directions of movements for storm A at 24h of Exps. 5-7. In Exp. 5 both the beta drift and interaction (both the rotation and convergence are counted for) are strong, the movement of the storm is mostly due south as evident in Fig. 15. In Exp. 6, the beta drift is weaker but the interaction is the strongest, the movement is nearly along the vector of the interaction. In Exp. 7, the beta effect is strong while the interaction is weak, results in a slow movement of the strom away from storm B.

4. SUMMARY

The interactions between two mesoscale cyclonic vortices in the absence of large scale winds have been investigated with a nondivergent, barotropic model and a three-dimensional model. Model results indicate that the interactions between a nondivergent barotropic vortex pair are very different from those observed between a tropical cyclone pair, and that our three-dimensional simulations agree with the observed Fujiwhara phenomenon.

Two types of vortex pairs with various initial separation distances have been tested with the nondivergent, barotropic model. No mutual attraction is found in any of the cases tested. The curvature of the mutually induced rotation depends on the radial profile of swirl winds (or vorticities) of each vortex, the speed of mutually induced motion is a function of separation —— the closer the two vortices, the faster they move. This is quite understandable, because in such a nondivergent barotropic model the two vortices can only interact by advection. These numerical experiments suggest that the observed Fujiwhara phenomenon is caused by a more complex mechanism than just vorticity advection.

Our simulations with a three-dimensional model reproduce observed Fujiwhara effects. The trajectories of simulated strong-strong, weak-weak, and weak-strong tropical cyclone pairs on a constant-f plane all consist of cyclonic rotations and mutual attractions. The rotation rate between two strong tropical cyclones is generally faster than that between a weak pair. The rate of convergence of a weak pair *is not slower than* that between a strong pair.

Additional analyses show that as the tropical cyclone pair start to interact, there forms a mean circulation about the center of mass of the two storms as the pressure there decreases more than can be expected by simple advective merging. The development of the mean circulation, consisting of a cyclonic tangential flow and a inward radial flow, resembles the circulation in weak but intensifying tropical disturbances. The kinetic energy of this mean circulation grows by a factor of four in 72h in one experiment, while the kinetic energy of the circulations associated with individual tropical cyclone remains relatively unchanged. It suggests that the development of a mean circulation on the vertical-radial plane relative to the center of mass of the interacting storm pairs is crucial in generating the cyclonic mutual rotation and merging.

A simple analysis points out that the displacement of one tropical cyclone interacting with another is proportional to the combined strength of the vortex pair and inversely proportional to its own size and to the square of the separation distance. Our model results fit this description well except for cases when interacting storms become highly asymmetric about their own centers.

The latitudinal variation of the Coriolis parameter (beta effect) has a large influence on the trajectories of the interacting storm pairs. The beta effect causes a northwest shift and a faster merging of the two tropical cyclones of equal strength. The trajectories of two interacting tropical cyclones of equal strength have a northwest drift superposed on the symmetrical trajectories found on the constant-f plane. Observation studies showed that typhoon pairs sometimes drifted away from each other if there were strong shears in large scale flow (Liu and Wang, 1966; Dong and Neumann, 1982). This study indicated that differential beta drifts can also cause the two interacting tropical cyclones of different strength to diverge when the one initially located to the west is stronger.

These findings should not be accepted without caution because of several limitations of the numerical model. The model domain is perhaps too small for two tropical cyclones. In addition, the horizontal resolution of $\frac{1}{2}^{\circ}$ is only marginal for resolving realistically the smaller scale dynamics near the center. Being a uniform grid model, without decreasing the horizontal resolution, the model domain cannot be expanded due to limited computing resources. The cyclic boundary conditions created problems (as evident in Exp. 7) when two storms may have interacted with each other through the east-west boundaries. Perhaps the most serious limitation of our simulation is the heating prescribed <u>a prior</u> in the three-dimensional simulations, which may have masked the interactions between two adjacent tropical cyclones on the scale of cumulus convections. However, the development of the mean circulation about the center of mass of the two tropical cyclones occurs at very early stage of the interaction when the separation is still large. This suggests that the detailed characteristics of cumulus convection in individual storm may not be important in setting up the cyclic rotation and mutual attraction. The use of the prescribed heating was justifiable except at small separations where the divergent-convergent pattern in each storm may be modified due to the proximity of another one.

In future research, a parameterized convective heating should be utilized to investigate the abovementioned secondary effect of the cumulus convection. In addition, the parameterized heating may react to large scale winds in a nonlinear fashion. Therefore, the nonlinear effects of the large scale winds on the interactions of two tropical cyclones also ought to be studied. The question of what is the maximum separation distance for storm pair to interact is also left for future studies when numerical models of tropical cyclone cover a larger domain are constructed.

ACKNOWLEDGEMENTS

I thank Dr. Rangarao V. Madala for discussions and his help in utilizing his stabilized-error-vector-propagation solver program, and Dr. Darrell F. Strobel for reading and commenting on the manuscript. Dr. Richard A. Anthes critically reviewed an earlier version of the manuscript, Mr. Charles J. Neumann kindly provided me his unpublished paper (Dong and Neumann, 1982) and a copy of Fujiwhara (1931) paper. Ms. Shoba Yalamanchili typed the manuscript.

The research was supported by ONR Contracts N00014-18-C-2224 and N00014-82-C-2306.

REFERENCES

Adem, J., 1956: A series solution for the barotropic vorticity equation and its application in the study of atmospheric vortices. Tellus, 8, 364-372.

Adler, R. F., and E. B. Rodgers, 1977: Satellite-observed latent heat release in a tropical cyclone. Mon. Wea. Rev., 105, 956-963.

Anthes, R. A., 1971: A numerical model of the slowly varying tropical cyclones in isentropic coordinates. Mon. Wea. Rev., 99, 617-635.

Anthes, R. A., 1977: A cumulus parameterization scheme utilizing a one-dimensional cloud model. Mon. Wea. Rev., 105, 270-286.

Anthes, R. A., 1982: Tropical cyclones — Their evolution, structure and effects. meteorological monographs, American Meteorlogical Society, Boston, ISBN 9-933876-54-8.

Anthes, R. A. and J. E. Hoke, 1975: The effect of horizontal divergence and the latitudinal variation of the Coriolis parameter on the drift of a model hurricane. Mon. Wea. Rev., 103, 757-763.

Brand, S. 1970: Interaction of binary tropical cyclones of the western North Pacific Ocean. J. Appl. Meteor., 9, 433-441.

Chang, S. W., 1981: Test of a planetary boundary layer parameterization based on a generalized similarity theory in tropical cyclone models. Mon. Wea. Rev., 109, 843-853.

Chang, S. W., 1982: The orographic effects induced by an island mountain range on propagating tropcial cyclones. Mon. Wea. Rev., 110, 1255-1270.

Chang, S. W. and R. V. Madala, 1980: Numerical simulation of the influence of sea surface temperature on translating tropical cyclones. J. Atmos. Sci., 36, 2617-2630.

Fujiwhara, S., 1921: The natural tendency towards symmetry of motion and its application as a principle in meteorology. Quart. J. Roy. Meteor. Soc., 47, 287-293.

Fujiwhara, S., 1923: On the growth and decay of vortical systems. Quart. J. Roy. Meteor. Soc., 49, 75-104.

Fujiwhara, S., 1931: Short note on the behavior of two vortices, Proc. Physico-Mathematical Society of Japan, Third Series, 13, 106-110. Available from the Library of Congress, Washington, DC 20540 or the author S. W. Chang.

Haurwitz, B., 1951: The motion of binary tropical cyclones. Arch. Meteor. Geophys. Biolkin., A4, 73-86.

Hawkins, H. F. and D. T. Rubsam, 1968: Hurricane Hilda, 1964: I. Genesis, as revealed by satellite photographs, conventional and aircraft data. Mon. Wea. Rev., 96, 428-452.

Hoover, E. W., 1961: Relative motion of hurricane pairs. Mon. Wea. Rev., 89, 251-255.

Jarrall, J. D., S. Brand, and D. S. Nicklin, 1978: An analysis of western North Pacific tropical cyclone forecast errors. Mon. Wea. Rev., 106, 925-937.

Liu, D. L. amd S. T. Wang, 1966: Case study of interactions of Pacific Ocean typhoons. Quart. J. Weather Forecasting and Analysis (in Chinese). Available from the second author at the Department of Atmospheric Sciences, National Taiwan University, Taipei, Taiwan.

Madala, R. V., 1978: An efficient direct solver for separable and nonseparable elliptic equations. Mon. Wea. Rev., 106, 1735-1741.

Madala, R. V. and S. A. Piascek, 1975: Numerical simulation of asymmetric hurricane on a β-plane with vertical shear. Tellus, 27, 453-468.

Neumann, C. J., 1982: Trends in forecasting the tracks of Atlantic tropical cyclones. Bull. Amer. Meteor. Soc., 62, 1473-1485.

Rossby, C. G., 1948: On displacements and intensity changes of atmospheric vortices. J. Marine Res., 7, 175-187.

FIGURES

Figure 1: Surface isobaric analyses at ooooZ on Sept. 15-20, 1964 showing the rotation and merging of typhoons Kathy (K) and Marie (M). Isobars are plotted every 3 mb. (From Liu and Wang, 1966).

Figure 2: The radial distribution of relative vorticity for type A (solid) and type B vortex (dashed).

Figure 3: The trajectories of type A (solid lines) and type B (dashed lines) vortices at separation distances of 300, 400, 600, and 1000 km. The cross is the center of the domain. Time interval between two adjacent dots is 12h. Squares denote the initial vortex centers.

Figure 4: The vertical distribution of heating used in the model plotted on an arbitrary scale (solid), as compared with (T_c-T) for mean hurricane sounding produced by a one-dimensional cloud model (Anthes, 1977, Fig. 4).

Figure 5: The horizontal distribution of heating used in the model plotted on an arbitrary scale (solid), as compared with the observed radial distribution of rainfall rate in a typhoon (Adler and Rodgers, 1977, Fig. 5).

Figure 6: The radial distribution of the quasi-steady wind speeds in model layer six ($\bar{\sigma}$ = 0.85) and seven ($\bar{\sigma}$ = 0.963) generated by the stationary prescribed heating.

Figure 7: The surface pressure field at 24, 48, 72, 84, and 96h. Contour intervals are 4 mb, the outmost closed isobars are 1008 mb. Longtitudes are arbitrarily set.

Figure 8: The trajectories of storm centers in Exp. 1. Numbers on the curve denote times in hour.

Figure 9: As in Figure 8, except for Exp. 2.

Figure 10: The tangential and radial speeds of the two interacting tropical cyclones relative to their centers of mass in Exps. 1 and 2.

Figure 11: As in Fig. 8, except for Exp. 3.

Figure 12: The azimuthal mean radial (v_r), tangential (v_θ), and vertical velocity (w) of the wind fields relatives to the center of mass in Exp. 1 at 24, 48, 72 and 96h.

Figure 13: The development of the kinetic energy of the "mean" flow (solid) relative to the center of mass and the kinetic energy of the "eddy" associated with the two storm centers (dashed) in Exp. 1.

Figure 14: The rotational rates ω compared with $(v_A + v_B)^2/fL^2$.

Figure 15: The trajectories of the free drifting storm in Exp. 4 (Curve C) and of the two interacting storms in Exp. 5 (Curves a and B).

Figure 16: As in Fig. 15 except for Exps. 6 (solid lines with dots) and 7 (solid lines with squares).

Figure 17: Vectors showing schematically the force of interaction (I), beta drift (D), and the resultant movement (M) for tropical cyclones A at 24h of Exps. 5, 6, and 7.

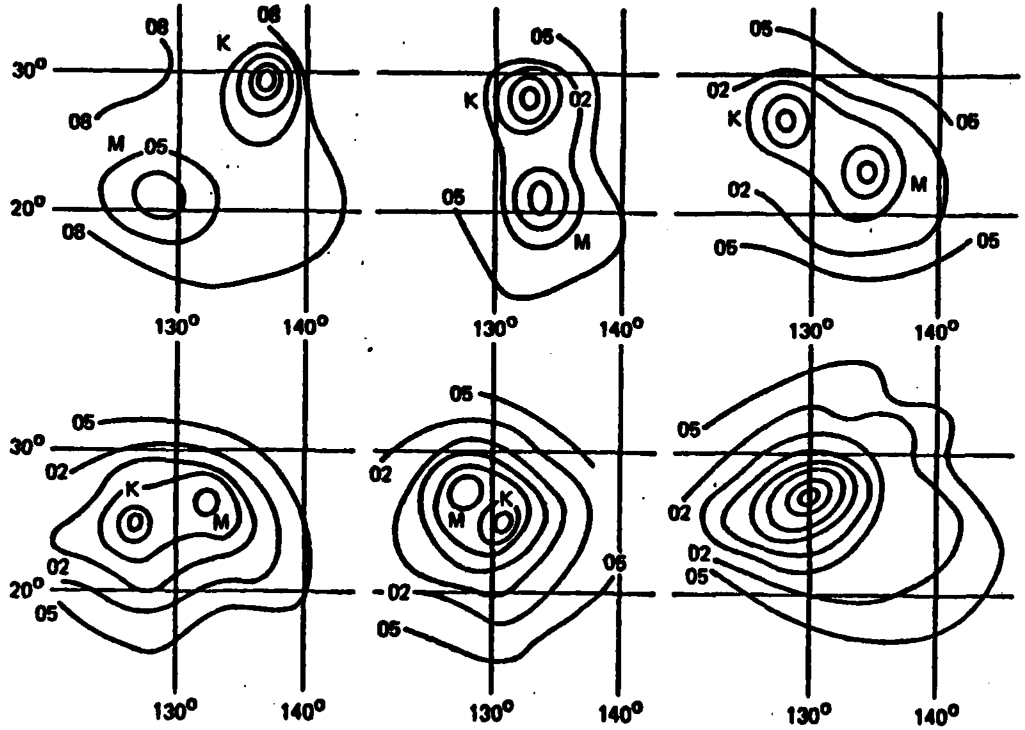

30°
20°
130°
140°
K
M
08
05
02

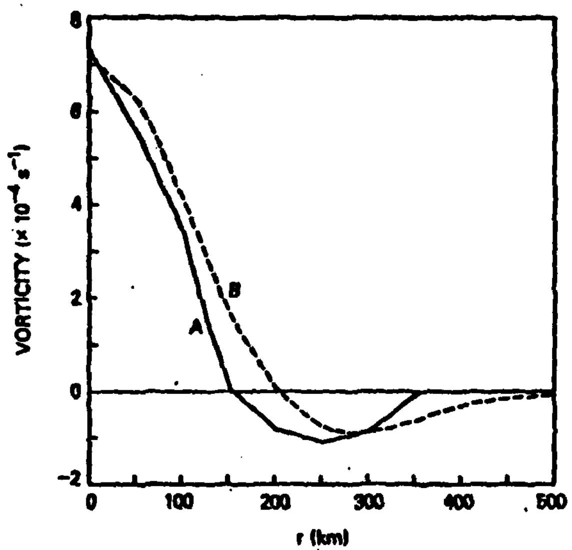

2

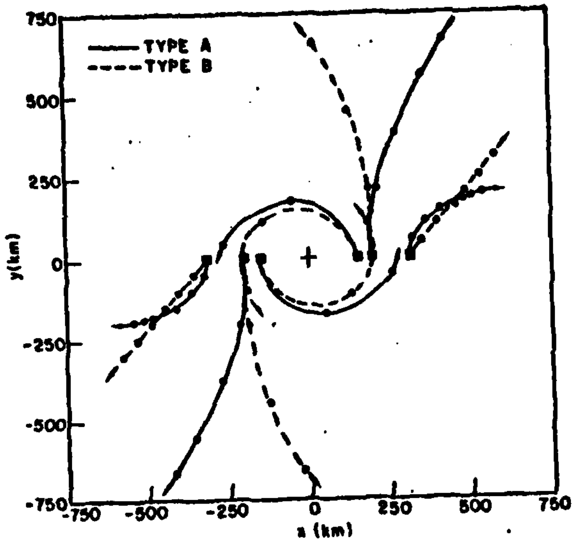

TYPE A
TYPE B
750
500
250
0
-250
-500
-750
y(km)
-750
-500
-250
0
250
500
750
x (km)

3

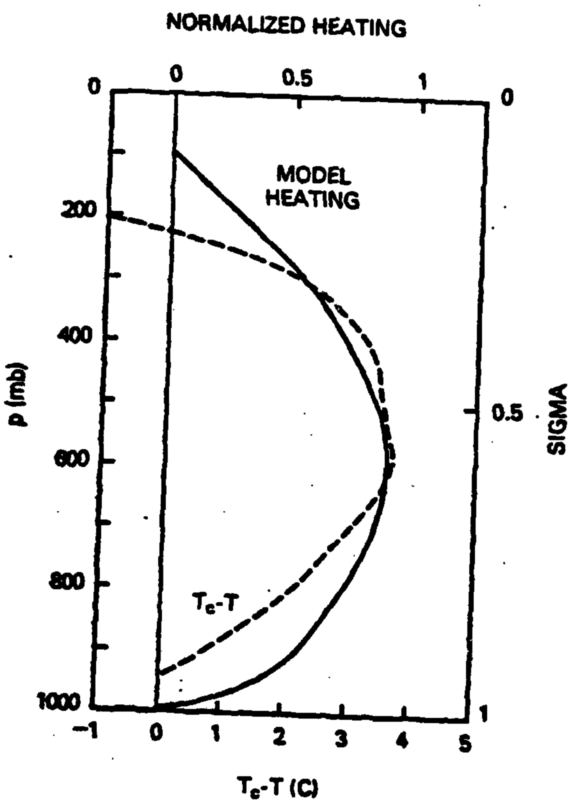

NORMALIZED HEATING
0
0.5
1
0
200
400
600
800
1000
0
0.5
1
MODEL
HEATING
Tc-T
p (mb)
SIGMA
−1
0
1
2
3
4
5
Tc-T (C)

4

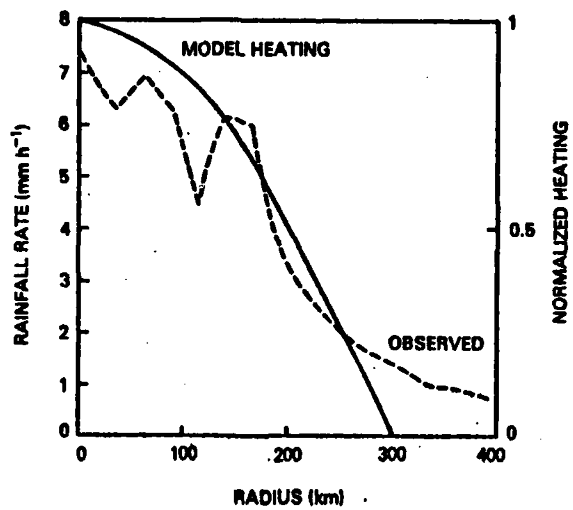
MODEL HEATING
OBSERVED
RAINFALL RATE (mm h^{-1})
NORMALIZED HEATING
RADIUS (km)
0
1
2
3
4
5
6
7
8
0.5
100
200
300
400

5

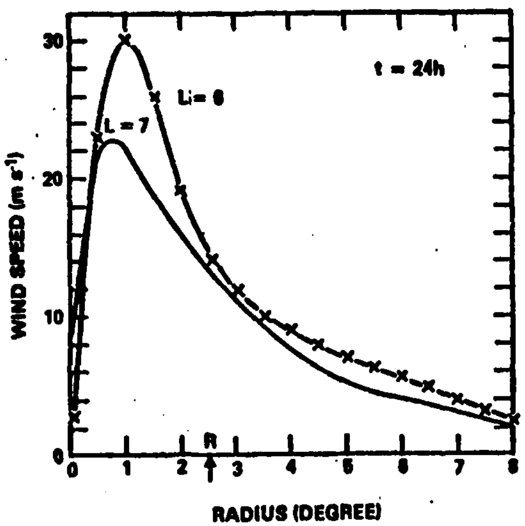

6

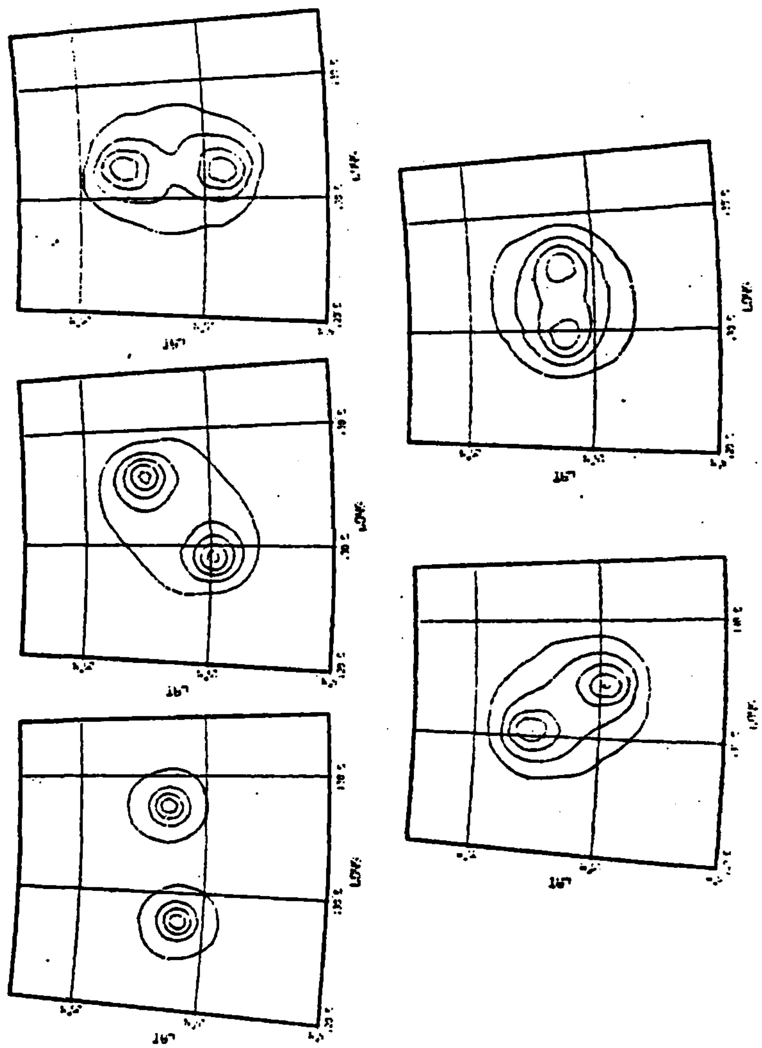

7

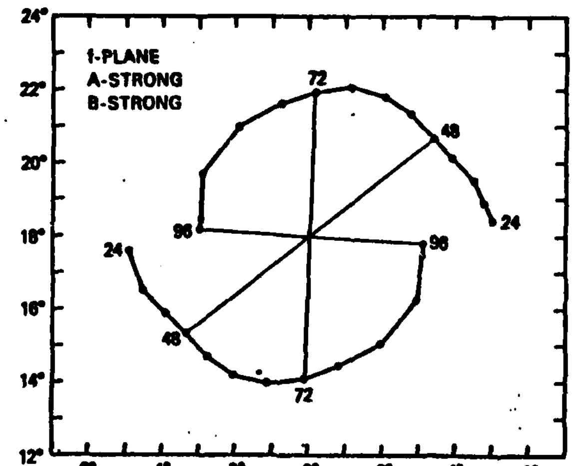
f-PLANE
A-STRONG
B-STRONG
72
48
24
96
96
24
48
72
24°
22°
20°
18°
16°
14°
12°
-6°
-4°
-2°
0°
2°
4°
6°

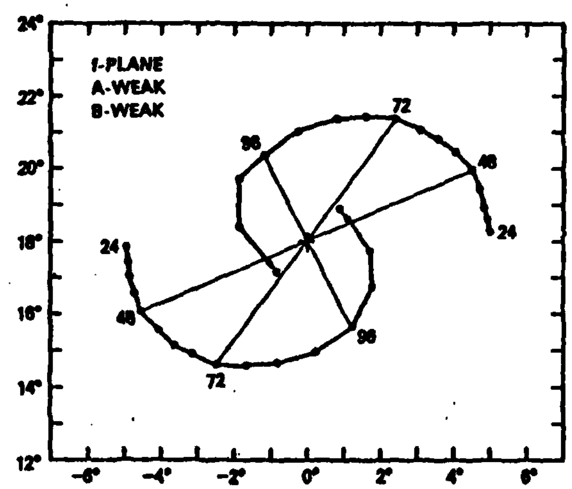

4

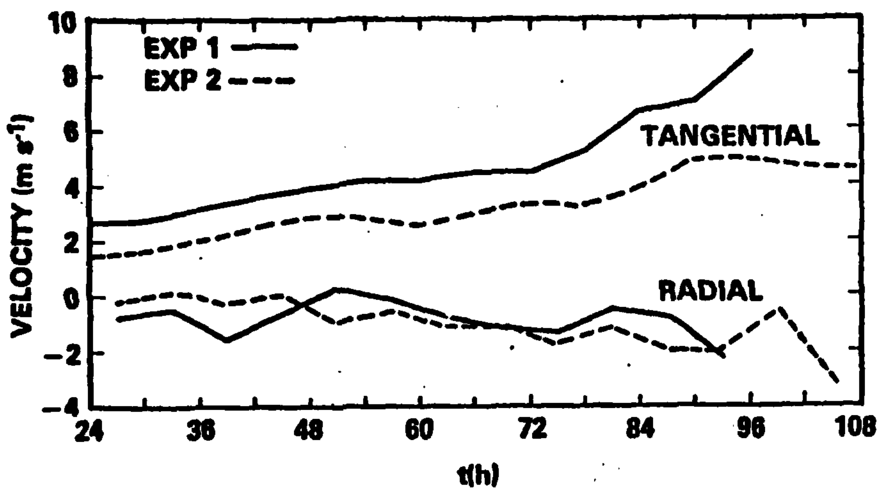

EXP 1
EXP 2
TANGENTIAL
RADIAL
VELOCITY (m s-1)
t(h)
10
8
6
4
2
0
−2
−4
24
36
48
60
72
84
96
108

10

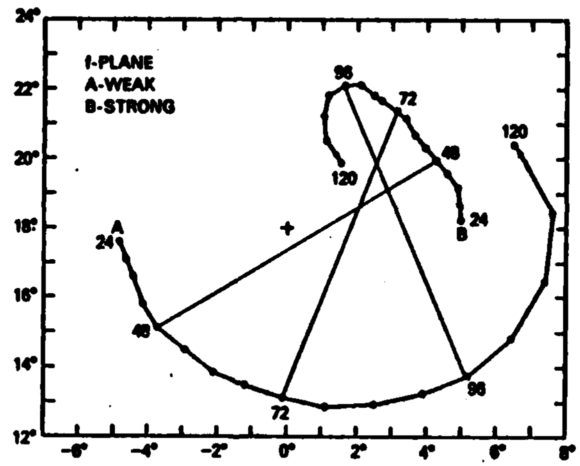
f-PLANE
A-WEAK
B-STRONG
24°
22°
20°
18°
16°
14°
12°
-6°
-4°
-2°
0°
2°
4°
6°
8°
A
24
48
72
96
120
B
24
48
72
96
120

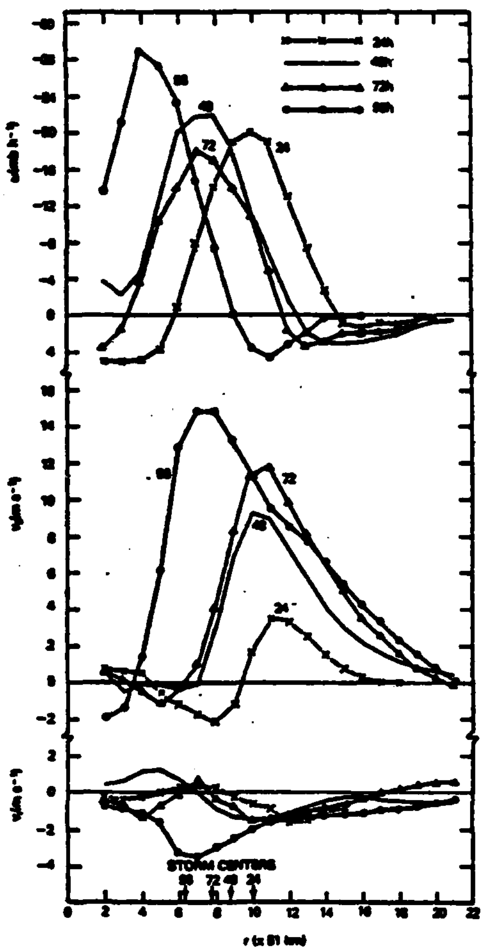
24h
48h
72h
96h
96
48
72
24
STORM CENTERS
96 72 48 24
r (x 81 km)

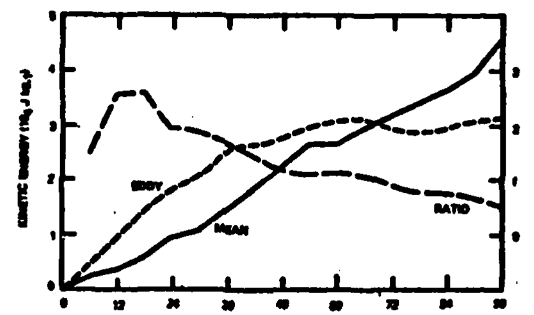
EDDY
MEAN
RATIO

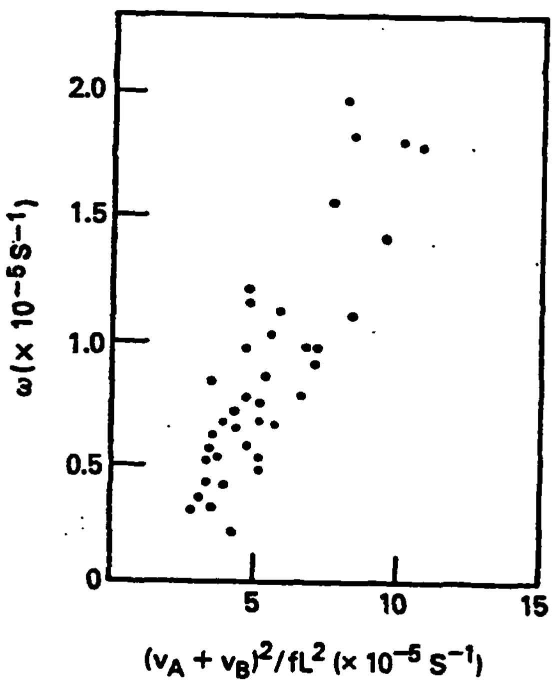

2.0
1.5
1.0
0.5
0
$\omega (\times 10^{-5} S^{-1})$
5
10
15
$(v_A + v_B)^2/fL^2\ (\times 10^{-5}\ S^{-1})$

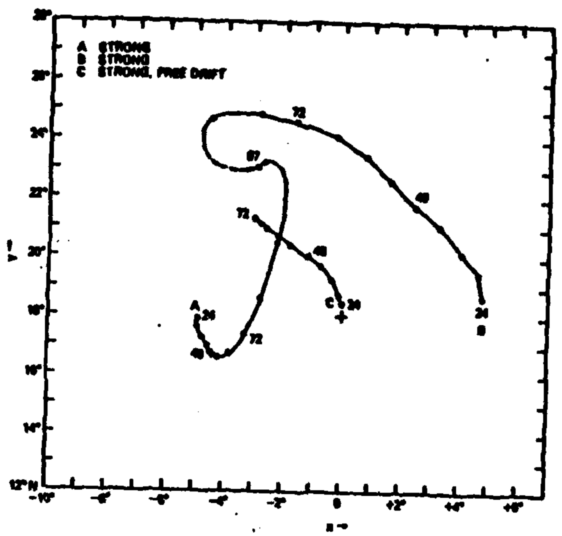

15

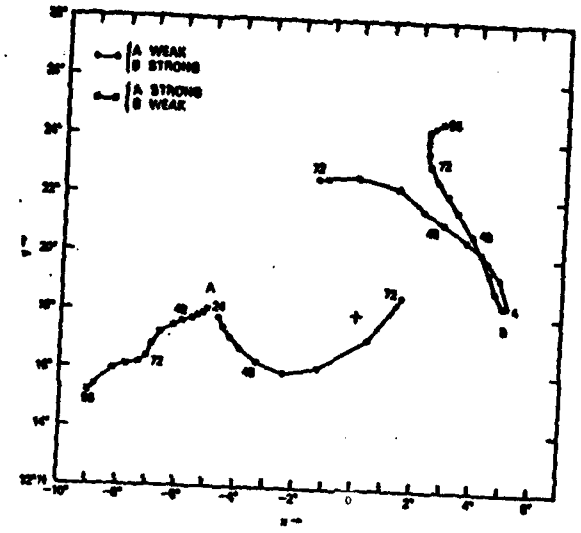

16

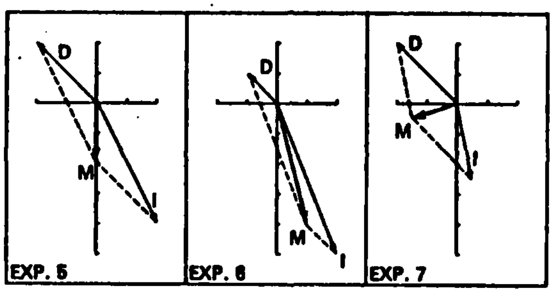
D
M
I
EXP. 5
D
M
I
EXP. 6
D
M
I
EXP. 7

APPENDIX II

AN AXISYMMETRIC MODEL FOR A NON-HYDROSTATIC BOUSSINESQ OCEAN

AN AXISYMMETRIC MODEL FOR A NON-HYDROSTATIC BOUSSINESQ OCEAN

Simon Wei-Jen Chang
Science Applications, Inc.
McLean, VA 22102

January 1983

CONTENTS

AN AXISYMMETRIC, NUMERICAL MODEL FOR A NON-HYDROSTATIC BOUSSINESQ OCEAN

1. GOVERNING EQUATIONS

The governing equations of the axisymmetric, non-hydrostatic, Boussinesq ocean model are

$$\frac{\partial u}{\partial t} + u\frac{\partial u}{\partial r} + w\frac{\partial u}{\partial z} = \frac{v^2}{r} + fv - \frac{1}{\rho_o}\frac{\partial p}{\partial r} + K_H\left(\nabla^2 u - \frac{u}{r^2}\right) + K_z\frac{\partial^2 u}{\partial z^2} \qquad (1\text{-}1)$$

$$\frac{\partial v}{\partial t} + u\frac{\partial v}{\partial r} + w\frac{\partial v}{\partial z} = -\frac{uv}{r} - fu + K_H\left(\nabla^2 v - \frac{v}{r^2}\right) + K_z\frac{\partial^2 v}{\partial z^2} \qquad (1\text{-}2)$$

$$\frac{\partial w}{\partial t} + u\frac{\partial w}{\partial r} + w\frac{\partial w}{\partial z} = -b - \frac{1}{\rho_o}\frac{\partial p}{\partial z} + K_H\nabla^2 w + K_z\frac{\partial^2 w}{\partial z^2} \qquad (1\text{-}3)$$

$$\frac{\partial b}{\partial t} + u\frac{\partial b}{\partial r} + w\frac{\partial b}{\partial z} = N_z^2 w + K_H\nabla^2 b + K_z\frac{\partial^2 b}{\partial z^2} \qquad (1\text{-}4)$$

where $\nabla^2 \equiv \frac{\partial^2}{\partial r^2} + \frac{1}{r}\frac{\partial}{\partial r}$, other symbols are listed in Appendix A. Above, the density anomaly b is defined according to

$$b = \frac{\rho - \rho_r(z)}{\rho_o}g, \qquad (1\text{-}5)$$

where $\rho_r(z)$ is a reference density and is a function of depth only. Brunt-Väisällä frequency N_z is defined as

$$N_z = \sqrt{\left(\frac{-g}{\rho_o}\frac{\partial \rho_r}{\partial z}\right)} \qquad (1\text{-}6)$$

Manuscript approved September 29, 1982.

The continuity equation is that of the incompressible fluid,

$$\frac{1}{r}\frac{\partial ur}{\partial r} + \frac{\partial w}{\partial z} = 0 \qquad (1\text{-}7)$$

2. THE MODEL GRID

It is determined that a fully staggered grid is most expedient for storage economy for a given spatial resolution. As shown in Fig. 1, the radial (u) and the tangential (v) velocities are defined at cross points, vertical velocities (w) are defined at open circle points, and the pressures (p) and density anomalies (b) are defined at blackened dot points. This grid system has the following advantages:

a) it saves storage for a given spatial resolution

b) it is very economical in terms of number of computational operations for the finite difference (FD) equations of (1-1) to (1-4).

c) it is very easy to specify the boundary conditions,

d) the pressure diagnostic equation, of the elliptic type, can be reduced to the standard form, and

e) there is no spatial separation of solutions on the grid.

In order to consistently index the grid points, we let index pair (ij) represent the i-th point in the r-direction and j-th point in the z-direction. In addition, m is the maximum number of points in the r-direction, and n, the maximum number of points in the z-direction. Therefore there are m x (n-1) points for radial and tangential velocities, (m-1) x n points for vertical velocities, and (m-1) x (n-1) points for mass distribution (b and p).

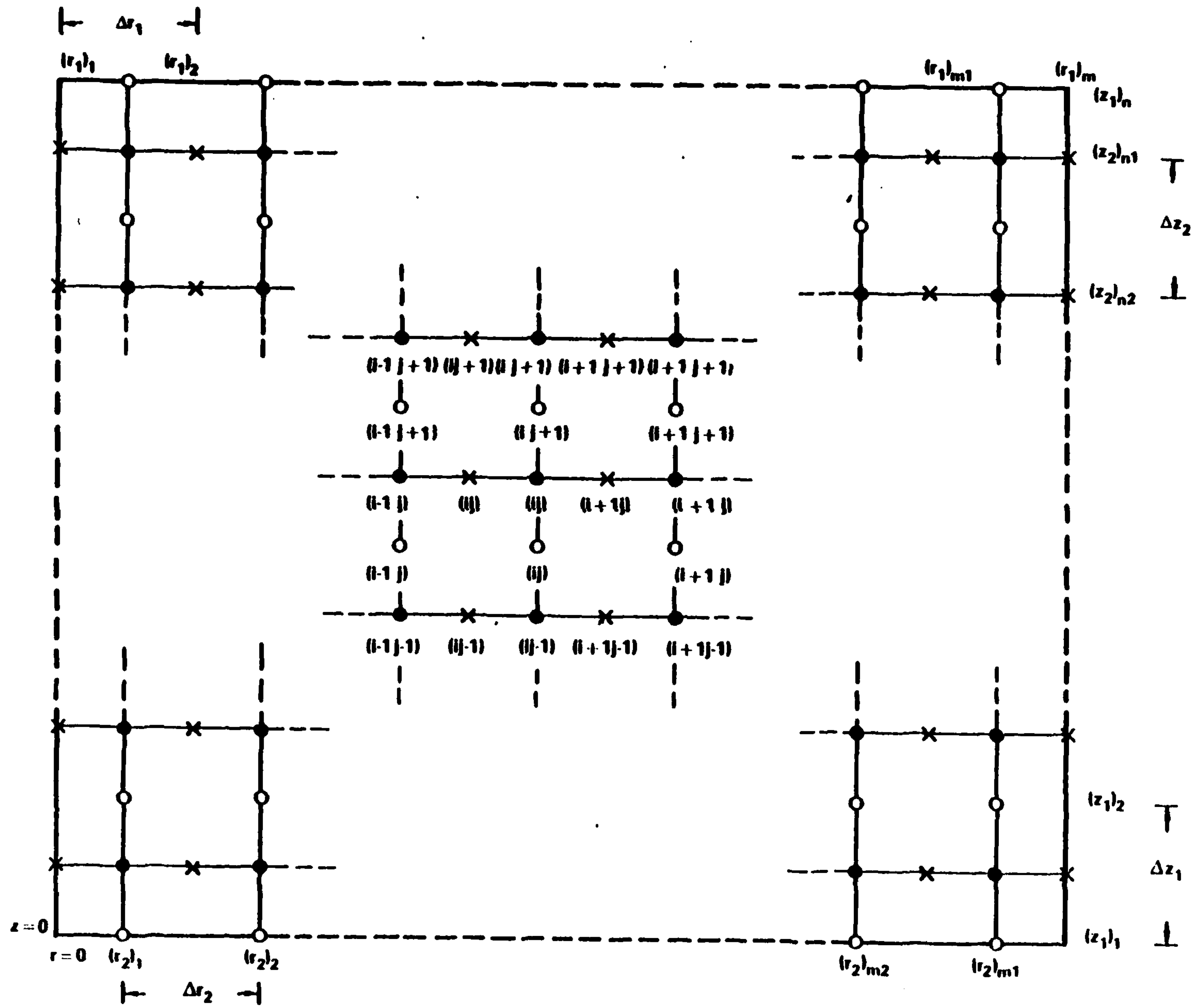

Fig. 1 The fully staggered grid system of the ocean model.

3. THE FINITE DIFFERENCE EQUATIONS

The leapfrog, or centered-in-time, integration scheme for the inviscid terms and the forward-in-time integration scheme for the viscous terms are used. The scheme is described as

$$\begin{Bmatrix} u^{t+\Delta t} \\ v^{t+\Delta t} \\ w^{t+\Delta t} \\ b^{t+\Delta t} \end{Bmatrix} = \begin{Bmatrix} u^{t-\Delta t} \\ v^{t-\Delta t} \\ w^{t-\Delta t} \\ b^{t-\Delta t} \end{Bmatrix} + 2\Delta t \begin{Bmatrix} \frac{\partial u^t}{\partial t} \\ \frac{\partial v^t}{\partial t} \\ \frac{\partial w^t}{\partial t} \\ \frac{\partial b^t}{\partial t} \end{Bmatrix} \qquad (3\text{-}1)$$

A second order, or centered-in-space, scheme is applied to derive the tendencies in (3-1) according to (1-1) ~ (1-4).

(a) <u>The Equation of Motion in r-direction</u>

$$\frac{\partial u^t_{ij}}{\partial t} = H^t_{ij} - \frac{1}{\rho_o} \frac{1}{(\Delta r_2)_i} (p_{ij} - p_{i-ij}) \qquad (3\text{-}2)$$

where

$$
\begin{aligned}
H_{ij}^{t} = -0.25 \Bigg[& \frac{1}{(\Delta r_1)_{i-1}} (u_{ij}^{t} + u_{i-1j}^{t})(u_{ij}^{t} - u_{i-1j}^{t}) \\
& + \frac{1}{(\Delta r_1)_i} (u_{i+1j}^{t} + u_{ij}^{t})(u_{i+1j}^{t} - u_{ij}^{t}) \\
& + \frac{1}{(\Delta z_2)_j} (w_{i-1j}^{t} + w_{ij}^{t})(u_{ij}^{t} - u_{ij-1}^{t}) \\
& + \frac{1}{(\Delta z_2)_{j+1}} (w_{ij+1}^{t} + w_{i-1j+1}^{t})(u_{ij+1}^{t} - u_{ij}^{t}) \Bigg] \\
& + v_{ij}^{t} \left[\frac{v_{ij}^{t}}{(r_1)_i} + f \right] \\
& + K_H \Bigg\{ \frac{1}{(\Delta r_2)_i} \Bigg[\frac{1}{(\Delta r_1)_i} (u_{i+1j}^{t-\Delta t} - u_{ij}^{t-\Delta t}) \\
& \qquad - \frac{1}{(\Delta r_1)_{i-1}} (u_{ij}^{t-\Delta t} - u_{i-1j}^{t-\Delta t}) \Bigg] \\
& + 0.5 \Bigg[\frac{1}{(r_2)_i (\Delta r_1)_i} (u_{i+1j}^{t-\Delta t} - u_{ij}^{t-\Delta t}) \\
& \qquad + \frac{1}{(r_2)_{i-1} (\Delta r_1)_{i-1}} (u_{ij}^{t-\Delta t} - u_{i-1j}^{t-\Delta t}) \Bigg] \\
& - \frac{u_{ij}^{t-\Delta t}}{(r_1)_i^2} \Bigg\} + \frac{K_z}{(\Delta z_1)_j} \Bigg[\frac{1}{(\Delta z_2)_{j-1}} (u_{ij+1}^{t-\Delta t} - u_{ij}^{t-\Delta t}) \\
& \qquad - \frac{1}{(\Delta z_2)_j} (u_{ij}^{t-\Delta t} - u_{ij-1}^{t-\Delta t}) \Bigg]
\end{aligned}
\qquad 3\text{-}3
$$

(b) The Equation of Motion in θ-direction

$$
\begin{aligned}
\frac{\partial v_{ij}^{t}}{\partial t} = -0.25 \Bigg[& \frac{1}{(\Delta r_1)_{i-1}}\left(u_{ij}^{t}+u_{i-1j}^{t}\right)\left(v_{ij}^{t}-v_{i-1j}^{t}\right) \\
& + \frac{1}{(\Delta r_1)_{i}}\left(u_{i+1j}^{t}+u_{ij}^{t}\right)\left(v_{i+1j}^{t}-v_{ij}^{t}\right) \\
& + \frac{1}{(\Delta z_2)_{j}}\left(w_{i-1j}^{t}+w_{ij}^{t}\right)\left(v_{ij}^{t}-v_{ij-1}^{t}\right) \\
& + \frac{1}{(\Delta z_2)_{j+1}}\left(w_{ij+1}^{t}+w_{i-1j+1}^{t}\right)\left(v_{ij+1}^{t}-v_{ij}^{t}\right) \Bigg] \\
& - u_{ij}^{t}\left[\frac{v_{ij}^{t}}{(r_1)_i} + f\right] \\
& + \frac{K_H}{(\Delta r_2)_i}\Bigg\{\Bigg[\frac{1}{(\Delta r_1)_i}\left(v_{i+1j}^{t-\Delta t}-v_{ij}^{t-\Delta t}\right) \\
& \qquad - \frac{1}{(\Delta r_1)_{i-1}}\left(v_{ij}^{t-\Delta t}-v_{i-1j}^{t-\Delta t}\right)\Bigg] \\
& + 0.5\Bigg[\frac{1}{(r_2)_i(\Delta r_1)_i}\left(v_{i+1j}^{t-\Delta t}-v_{ij}^{t-\Delta t}\right) \\
& \qquad + \frac{1}{(r_2)_{i-1}(\Delta r_1)_{i-1}}\left(v_{ij}^{t-\Delta t}-v_{i-1j}^{t-\Delta t}\right)\Bigg] \\
& - \frac{v_{ij}^{t-\Delta t}}{(r_1)_i^2}\Bigg\} + \frac{K_z}{(\Delta z_1)_j}\Bigg[\frac{1}{(\Delta z_2)_{j+1}}\left(v_{ij+1}^{t-\Delta t}-v_{ij}^{t-\Delta t}\right) \\
& \qquad - \frac{1}{(\Delta z_2)_j}\left(v_{ij}^{t-\Delta t}-v_{ij-1}^{t-\Delta t}\right)\Bigg]
\end{aligned}
\qquad (5\text{-}4)
$$

(c) The Equation of Motion in z-direction

$$\frac{\partial w_{ij}^{t}}{\partial t} = G_{ij}^{t} - \frac{1}{\rho_o (\Delta z_2)_j} (p_{ij} - p_{ij-1}) \qquad (3\text{-}5)$$

where

$$\begin{aligned}
G_{ij}^{t} = -0.25 \Bigg[& \frac{1}{(\Delta r_2)_i} (u_{ij}^{t} + u_{ij-1}^{t}) (w_{ij}^{t} - w_{i-1j}^{t}) \\
& + \frac{1}{(\Delta r_2)_{i+1}} (u_{i+1j}^{t} + u_{i+1j-1}^{t}) (w_{i+1j}^{t} - w_{ij}^{t}) \\
& + \frac{1}{(\Delta z_1)_{j-1}} (w_{ij-1}^{t} + w_{ij}^{t}) (w_{ij}^{t} - w_{ij-1}^{t}) \\
& + \frac{1}{(\Delta z_1)_j} (w_{ij+1}^{t} + w_{ij}^{t}) (w_{ij+1}^{t} - w_{ij}^{t}) \Bigg] \\
& - 0.5 (b_{ij}^{t} + b_{ij-1}^{t}) \\
& + K_H \Bigg\{ \frac{1}{(\Delta r_1)_i} \Bigg[\frac{1}{(\Delta r_2)_{i+1}} (w_{i+1j}^{t-\Delta t} - w_{ij}^{t-\Delta t}) \\
& \qquad - \frac{1}{(\Delta r_2)_i} (w_{ij}^{t-\Delta t} - w_{i-1j}^{t-\Delta t}) \Bigg] \\
& + 0.5 \Bigg[\frac{1}{(r_1)_{i+1} (\Delta r_2)_{i+1}} (w_{i+1j}^{t-\Delta t} - w_{ij}^{t-\Delta t}) \\
& \qquad + \frac{1}{(r_1)_i (\Delta r_2)_i} (w_{ij}^{t-\Delta t} - w_{i-1j}^{t-\Delta t}) \Bigg] \Bigg\}
\end{aligned}$$

$$+ \frac{K_z}{(\Delta z_2)_j}\left[\frac{1}{(\Delta z_1)_j}(w^{t-\Delta t}_{ij+1} - w^{t-\Delta t}_{ij}) - \frac{1}{(\Delta z_1)_{j-1}}(w^{t-\Delta t}_{ij} - w^{t-\Delta t}_{ij-1})\right] \quad (3\text{-}6)$$

(d) <u>The Thermodynamic Equation</u>

$$\frac{\partial b^t_{ij}}{\partial t} = -0.5\left[\frac{u^t_{ij}}{(\Delta r_2)_i}(b^t_{ij} - b^t_{i-1j}) + \frac{u^t_{i+1j}}{(\Delta r_2)_{i+1}}(b^t_{i+1j} - b^t_{ij})\right.$$

$$\left. + \frac{w^t_{ij}}{(\Delta z_2)_j}(b^t_{ij} - b^t_{ij-1}) + \frac{w_{ij+1}}{(\Delta z_2)_{j+1}}(b^t_{ij+1} - b^t_{ij})\right]$$

$$+ 0.5\ (w^t_{ij+1} + w^t_{ij})\ N^2_z$$

$$+ K_H \left\{\frac{1}{(\Delta r_1)_i}\left[\frac{1}{(\Delta r_2)_{i+1}}(b^{t-\Delta t}_{i+1j} - b^{t-\Delta t}_{ij})\right.\right.$$

$$\left. - \frac{1}{(\Delta r_2)_i}(b^{t-\Delta t}_{ij} - b^{t-\Delta t}_{i-1j})\right]$$

$$+ 0.5\left[\frac{1}{(r_1)_{i+1}(\Delta r_2)_{i+1}}(b^{t-\Delta t}_{i+1j} - b^{t-\Delta t}_{ij})\right.$$

$$\left.\left. + \frac{1}{(r_1)_i(\Delta r_2)_i}(b^{t-\Delta t}_{ij} - b^{t-\Delta t}_{i-1j})\right]\right\}$$

$$+ \frac{K_z}{(\Delta z_1)_j}\left[\frac{1}{(\Delta z_2)_{j+1}}(b^{t-\Delta t}_{ij+1} - b^{t-\Delta t}_{ij})\right.$$

$$\left. - \frac{1}{(\Delta z_2)_j}(b^{t-\Delta t}_{ij} - b^{t-\Delta t}_{ij-1})\right] \quad (3\text{-}7)$$

4. DERIVATION OF THE DIAGNOSTIC EQUATION FOR PRESSURE

The nonhydrostatic pressure at time t is needed to compute the pressure gradient forces in (3-2) and (3-5). To "recover" the pressure from the motion fields, we make use of the continuity equation by differentiating (1-7) with time we get

$$\frac{1}{r}\frac{\partial}{\partial r} r \frac{\partial u}{\partial t} + \frac{\partial}{\partial z}\frac{\partial w}{\partial t} = 0 ,$$

which can be written in finite difference form for a mass point ij as

$$\frac{1}{\frac{1}{2}\left[(r_1)_i + (r_1)_{i+1}\right](\Delta r_1)_i}\left[(r_1)_{i+1}\frac{\partial u^t_{i+1j}}{\partial t} - (r_1)_i\frac{\partial u^t_{ij}}{\partial t}\right]$$

$$+ \frac{1}{(\Delta z_1)_j}\left[\frac{\partial w^t_{ij+1}}{\partial t} - \frac{\partial w^t_{ij}}{\partial t}\right] = 0 \qquad (4\text{-}1)$$

Let $\quad c_i = (r_1)_{i+1}\Big/\left\{\frac{1}{2}\left[(r_1)_i + (r_1)_{i+1}\right](\Delta r_1)_i\right\}$,

$$(4\text{-}2)$$

and $\quad a_i = (r_1)_i\Big/\left\{\frac{1}{2}\left[(r_1)_i + (r_1)_{i+1}\right](\Delta r_1)_i\right\}$

Substituting (3-2), (3-5) and (4-2) into (4-1), we have

$$c_i H^t_{i+1j} - \frac{1}{\rho_o}\frac{c_i}{(\Delta r_2)_{i+1}}(p_{i+1j} - p_{ij}) - a_i H^t_{ij}$$

$$+ \frac{1}{\rho_o}\frac{a_i}{(\Delta r_2)_i}(p_{ij} - p_{i-1j}) + \frac{1}{(\Delta z_1)_j} G^t_{ij-1} - \frac{1}{(\Delta z_1)_j} G^t_{ij}$$

$$- \frac{1}{\rho_o (\Delta z_1)_j (\Delta z_2)_{j+1}} (p_{ij+1} - p_{ij})$$

$$+ \frac{1}{\rho_o (\Delta z_1)_j (\Delta z_2)_j} (p_{ij} - p_{ij-1}) = 0$$

After some rearrangements, we get

$$- \frac{c_i}{(\Delta r_2)_{i+1}} p_{i+1j} - \frac{a_i}{(\Delta r_2)_i} p_{i-1j}$$

$$- \frac{1}{(\Delta z_1)_j (\Delta z_2)_j} p_{ij-1} - \frac{1}{(\Delta z_1)_j (\Delta z_2)_{j+1}} p_{ij+1}$$

$$+ \left[\frac{c_i}{(\Delta r_2)_{i+1}} + \frac{a_i}{(\Delta r_2)_i} + \frac{1}{(\Delta z_1)_j (\Delta z_2)_{j+1}} + \frac{1}{(\Delta z_1)_j (\Delta z_2)_j}\right] p_{ij}$$

$$= \rho_o \left[- c_i H^t_{i+1j} + a_i H^t_{ij} - \frac{1}{(\Delta z_1)_j} G^t_{ij+1} + \frac{1}{(\Delta z_1)_j} G^t_{ij}\right] \quad (4\text{-}3)$$

Now let F_{ij} = RHS of (4-3),

$$CX_i = \frac{c_i}{(\Delta r_2)_{i+1}} = (r_1)_{i+1} \Big/ \left\{ \frac{1}{2}\left[(r_1)_i + (r_1)_{i+1}\right] (\Delta r_1)_i (\Delta r_2)_{i+1} \right\} ,$$

$$AX_i = \frac{a_1}{(\Delta r_2)_i} = (r_1)_i \Big/ \left\{ \frac{1}{2}\left[(r_1)_i + (r_1)_{i-1}\right] (\Delta r_1)_i (\Delta r_2)_i \right\} ,$$

$$CZ_j = 1/[(\Delta z_1)_j (\Delta z_2)_{j+1}] ,$$

$$AZ_j = 1/[(\Delta z_1)_j (\Delta z_2)_j] \text{ , and}$$

$$BB_{ij} = - CX_i - AX_i - CZ_j - AZ_j \qquad (4-4)$$

We obtain the standard form of an elliptic equation in FD form

$$AX_i p_{i-1j} + AZ_j p_{ij-1} + BB_{ij} p_{ij} + CX_i p_{i+1j} + CZ_j p_{ij+1} = F_{ij} \qquad (4-5)$$

Equation (4-5) can be solved numerically by the SEVP solver (Madala, 1978), providing the boundary conditions are properly posed.

The conditions for the four boundaries are determined according to the following assumptions:

(a) At $(r_1)_i = (r_1)_1 = 0$, the natural condition for the cylindrical coordinates calls for $u = v = 0 = \partial u/\partial t = \partial v/\partial t$, the gradient balance requires that $(\partial P/\partial r)_{r=0} = 0$. Therefore an extra column of P is needed

$$P_{oj} = P_{1j} \qquad (4-6)$$

(b) At $(r_1)_i = (r_1)_m$, assuming both the horizontal divergence and the vorticity are continuous, i.e., $\frac{\partial}{\partial r} \frac{1}{r} \frac{\partial ur}{\partial r} = 0$ and $\frac{\partial}{\partial r} \frac{1}{r} \frac{\partial vr}{\partial r} = 0$. These lead to

$$
\begin{aligned}
u_{mj} &= b_a u_{m1j} + b_b[(r_1)_{m1} u_{m1j} - (r_1)_{m2} u_{m2j}] \\
v_{mj} &= b_a v_{m1j} + b_b[(r_1)_{m1} v_{m1j} - (r_1)_{m2} v_{m2j}]
\end{aligned}
\qquad (4\text{-}7)
$$

where $b_a = (r_1)_{m1}/(r_1)_m$, and

$$b_b = [(r_1)_{m1}+(r_1)_m](\Delta r_1)_{m1}/\left\{(\Delta r_1)_{m2}[(r_1)_{m1}+(r_1)_{m2}]\right\}$$

Note that if b_b is set equal to zero, (4-7) describes a non-divergent and zero-vorticity boundary condition at $r = (r_1)_m$. Once v_{mj} is determined, a gradient balance at $r = (r_1)_m$ requires

$$\rho_o v_{mj} \left[\frac{v_{mj}}{(r_1)_m} + f\right] = \frac{1}{(\Delta r_2)_m} (p_{mj} - p_{m-1j})$$

or

$$p_{mj} = p_{m-1j} + \rho_o (\Delta r_2)_m v_{mj} \left[\frac{v_{mj}}{(r_1)_m} + f\right] \qquad (4\text{-}8)$$

where a column of dummy points p_{mj} has been introduced for computational purposes. The second part of the RHS of (4-8) is thus the forcing function at $(r_1)_m$ for the elliptic equation (4-5).

(c) At the bottom, $w_{i1} = \frac{\partial}{\partial t} w_{i1} = 0$. Substituting these into the continuity equation (4-1), we get

$$\frac{1}{\frac{1}{2}(r_1)_i + (r_i)_{i-1}(\Delta r_1)_i}\left[(r_1)_{i+1}\frac{\partial u^t_{i+11}}{\partial t} - (r_1)_i\frac{\partial u^t_{i1}}{\partial t}\right]$$

$$+ \frac{1}{(\Delta z_1)_1}\frac{\partial w^t_{i2}}{\partial t} = 0 \ . \tag{4-9}$$

Following the same deduction between (4-1) and (4-5), we get an expression similar to (4-5) with the second team on the LHS and G_{i1} in the RHS absent. Thus, P_{i1} can be obtained by the same SEVP solver by setting $CZ_1 = 0$ and $G_{i1} = 0$.

(d) At top $w_{in} = \partial/\partial t\ w_{in} = 0$. Following the same line of reasoning as in (c), we obtain P_{in} by solving (4-5) with $CZ_n\ P_{in+1} = 0$ and $G_{in} = 0$.

In summary, the elliptic pressure diagnostic equation (4-4) is to be solved with the following boundary conditions

1) At $r = 0$ $\quad P_{oj} = P_{1j}$ $\quad$ i.e., (4-6)
2) At $r = (r_1)_m$ $\quad P_{mj} = P_{m-1j}$ + function (v_{mj}) (4-8)
3) At $z = 0$ $\quad AZ_1 = 0$ and $G_{i1} = 0$
4) At $z = (z_1)_n$ $\quad CZ_n = 0$ and $G_{in} = 0$

LIST OF SYMBOLS

AX_i	an array of constants, varying only in r-direction, defined by (4-4), used in (4-5)
AZ_j	an array of constants, varying only in z-direction defined by (4-4), used in (4-5)
a_i	an array of constants related to r_1 and Δr_1 used in (4-2)
BB_{ij}	an array of constants, used in (4-5)
b	density anomalies, defined in (1-5), cm s^{-2}
CX_i	an array of constants, varying only in r-direction, defined by (4-4), used in (4-5)
CZ_j	an array of constants, varying only in z-direction, defined by (4-4), used in (4-5)
c_i	an array of constants, related to r_1 and Δr_1, used in (4-5)
f	Coriolis parameter, s^{-1}
g	gravitational acceleration, cm s^{-2}
i	an index, denoting i-th point in r-direction
j	an index, denoting j-th point in z-direction
K_H	horizontal diffusion coefficient, cm^2 s^{-1}
K_Z	vertical diffusion coefficient, cm^2 s^{-1}
LHS	left hand side
m	the maximum number of grid points in r-direction, upper bound of i

m_1	m-1
m_2	m-2
N_z	Brunt-Väisällä frequency, s^{-1}
n	the maximum number of grid points in z-direction, upper bound of j
n_1	n-1
n_2	n-2
p	pressure, dyne cm^{-2}
RHS	right hand side
r	radius, cm
r_1	radii of momentum points, cm
r_2	radii of mass points, cm
Δr_1	distance between two horizontally adjacent momentum points, cm
Δr_2	distance between two horizontally adjacent mass points, cm
SEVP	stabilized error vector propagation
t	time, s
Δt	time interval, s
u	radial velocity, cm s^{-1}
v	tangential velocity, cm s^{-1}
w	vertical velocity, cm s^{-1}
z	height from ocean bottom, cm
z_1	heights of circle points, cm
z_2	heights of cross and dot points, cm

Δz_1	distance between two vertically adjacent circle points, cm
Δz_2	distance between two vertically adjacent cross or dot points
ρ	density, g cm^{-3}
ρ_o	a constant density, 1 g cm^{-3}
ρ_r	a reference density, varying only in z-direction, g cm^{-3}

ACKNOWLEDGMENTS

Discussions with Dr. R. V. Madala on the SEVP solver and the skillful typing of Mrs. Doris Beechum and Mrs. Judy Staudinger are greatly appreciated.

REFERENCE

Madala, R. V., 1978: An Efficient Direct Solver for Separable and Non-Separable Elliptic Equations. Month Weather Review, 106, 1735-1741.

APPENDIX A — FORTRAN CODE FOR THE NON—HYDROSTATIC MODEL

A listing of FORTRAN code of the ocean model. The major functions of the main program and subroutines are as follows:

OCEAN	main program, calls all subroutines, manages job flow, controls input/output.
INIT	sets up independent variables, defines constants
START	defines initial conditions
PUTOUT	gets various fields ready for output
MAP	prints
ADVECT	computes all inviscous terms, except for the pressure gradient forces
DIFF	computes horizontal and vertical diffusions
PRESS	solves the pressure diagnostic equations and computes the pressure gradient forces, appears only in the non-hydrostatic version
MATINV	inverts matrices
BSM1	
BSM2	
BSM3	
FRWRD	matches forward
BOUNDV	sets outer boundary conditions for momentum
CHECK	checks if the time step is linearly stable.

Used in SEVP method

APPENDIX B — FORTRAN CODE FOR THE HYDROSTATIC MODEL

The hydrostatic version of the model can be obtained by simplifying the non-hydrostatic version. In the hydrostatic version, the equation of motion in z-direction (1-3) is reduced to the hydrostatic equation

$$-\frac{1}{\rho_o}\frac{\partial p}{\partial z} = b \tag{B-1}$$

Instead of solving the elliptic equation (4-5), the pressure p is thus obtainable by vertically integrating (B-1). The vertical velocity w can also be computed by vertically integrating the continuity equation (1-7).

The FD forms of (B-1) and (1-7) are, respectively,

$$p_{ij} = p_{ij-1} - 0.5\ \rho_o(\Delta z_r)_j\ (B^t_{ij} + B^t_{ij-1}) \tag{B-2}$$

$$w_{ij} = w_{ij} + \frac{\left[(r_1)_{i+1}\ u^t_{i+1j-1} - (r_1)_i\ u^t_{ij-1}\right](\Delta z_1)_j}{0.5\ (\Delta r_1)_i\ \left[(r_1)_{i+1} + (r_1)_i\right]} \tag{B-3}$$

CARD IMAGE FILE EDITOR(CIFER) -- VERSION 05.29 DATE=10/26/82   TIME=14:12:12:09

<<SPLIT OCEANO,SOURCO,PRINT,SEC

```
      PROGRAM OCEAN
      PARAMETER M=21,N=21
      PARAMETER M1=M-1,M2=M-2,N1=N-1,N2=N-2
      PARAMETER ND=2*M*N1+M1*N+M1*N1
      DIMENSION DATA1(ND),DATA2(ND),DATA3(ND)
      COMMON/ONE/VR1(M,N1),VT1(M,N1),VZ1(M1,N),B1(M1,N1),VR2(M,N1),
     1           VT2(M,N1),VZ2(M1,N),B2(M1,N1),VR3(M,N1),VT3(M,N1),
     2           VZ3(M1,N),B3(M1,N1),P(M1,N1)
      EQUIVALENCE (DATA1,VR1),(DATA2,VR2),(DATA3,VR3)
      DATA DATA1/ND*0./,DATA2/ND*0./,DATA3/ND*0./
      COMMON/TWO/R1(M),R2(M1),DR1(M1),DR2(M),Z1(N),Z2(N1),DZ1(N1),DZ2(N)
      COMMON/THR/RHO,WPER(N1),BV2(N),ALPHA,BNDA,BNDB,CORI,G,HK(M),ZK(N)
      COMMON/FOR/DELT,XTIME,ITIME,ISTEP,ISMO,ITAPE,TBV
      CALL INDUMP
  100 FORMAT(I4)
      READ(5,100)ITIME
      READ(5,100)ITER
      READ(5,100)IOUT
      READ(5,100)ISMO
      ISTEP=0
      READ(5,100)ITAPE
      CALL INIT
      IF(ITIME.EQ.0)GO TO 10
C
C                      CONTINUED INTEGRATION FROM A HISTORY TAPE
C
      READ(1)ITIME,DATA1,DATA2,P
      GO TO 20
   10 CALL START
   20 XTIME=ITIME*3600.
C
C                      PRINT OUT INITIAL FIELDS
C
      CALL PUTOUT
      IF(ITER.EQ.0)STOP
      DO 90 ISTEP=1,ITER
C
C                   COMPUTE ALL INVISCID TERMS
C
      CALL ADVECT
C
C                      COMPUTE VISCOUS TERMS
C
      CALL DIFF
C
C                      AND ADD PRESSURE GRADIENT FORCES TO TENDENCIES
C                      DIAGNOSE (RECOVER) THE PRESSURE FIELD
C
      CALL PRESS
C
C                      MARCHING IN TIME
C                      FIRST TIME STEP IS FORWARD IF START IS CALLED
C
      IF(ISTEP.EQ.1.AND.ITIME.EQ.0)DELT=0.5*DELT
      CALL FORWD
      IF(ISTEP.EQ.1.AND.ITIME.EQ.0)DELT=2.*DELT
C
C                      DEFINE BOUNDARY VALUES FOR VELOCITY
C
      CALL BOUNDV
C
C                      CHECK IF DELT IS STABLE
CC
      CALL CHECK
      XTIME=XTIME+DELT
      ITIME=XTIME/3600.
C
C                      PRINT OUT RESULTS EVERY IOUT STEPS
C
      IF(MOD(ISTEP,IOUT).EQ.0)CALL PUTOUT
C
C                      WRITE HISTORY TAPE EVERY ITAPE STEPS
C
      IF(MOD(ISTEP,ITAPE).EQ.0)WRITE(2)ITIME,DATA1,DATA2,P
   90 CONTINUE
      STOP
      END
```

CARD IMAGE FILE EDITOR(CIFEM) -- VERSION 05.29 DATE=10/26/82 TIME=14:12:12:99

*** MEMBER INIT

```
      SUBROUTINE  INIT
      PARAMETER M=21,N=21
      PARAMETER M1=M-1,M2=M-2,N1=N-1,N2=N-2
      COMMON/ONE/VR1(M,N1),VT1(M,N1),VZ1(M1,N),B1(M1,N1),VR2(M,N1),
     1          VT2(M,N1),VZ2(M1,N),B2(M1,N1),VR3(M,N1),VT3(M,N1),
     2          VZ3(M1,N),B3(M1,N1),P(M1,N1)
      COMMON/TWO/R1(M),R2(M1),DR1(M1),DR2(M),Z1(N),Z2(N1),DZ1(N1),DZ2(N)
      COMMON/THR/RHO,RHOR(N1),BV2(N),ALPHA,BNDA,BNDR,CORI,G,RK(M),ZK(N)
      COMMON/FOR/DELT,XTIME,ITIME,ISTEP,ISMO,ITAPE,TBV
      PARAMETER MP=M+1,NP=N+1
      PARAMETER NBLK=2,NBLK1=NBLK-1
      PARAMETER MP1=MP-1,MP2=MP-2,NP1=NP-1,NP2=NP-2
      REAL*8 RCOR,RINV,RINV1,RTILDA
      COMMON/EVP/RINV(MP2,MP2,NBLK),RINV1(MP2,MP2,NBLK1),RCOR(MP,3),
     1          RTILDA(MP2),F(MP,NP),NBSIZ2(NBLK),IS(NBLK),SUMF(NBLK),
     2          IE(NBLK),F11(MP),F1N(MP),F21(NP),F2M(NP),AX(MP),AY(NP),
     3          BB(MP,NP),CX(MP),CY(NP)
C
C               INITIALIZE ALL DEPENDENT VARIABLES AND CONSTANTS
C
C
C                ALPHA IS THE NONDIMENSIONAL SMOOTHING COEF.
C                FOR TIME SMOOTHING IN SUBROUTINE FRWRD
C
      DELT=900.
      ALPHA=0.10
      G=980.
      LAT=30
      CORI=2.*7.2722E-5*SIN(LAT*3.14159/180.)
C
C                DEFINE RADII AT GRID POINTS AND ALL GRID INTERVALS
C
      DO 10 I=1,M1
   10 DR1(I)=20.E5
      R1(1)=0.
      DO 20 I=2,M
   20 R1(I)=R1(I-1)+DR1(I-1)
      DO 30 I=1,M1
   30 R2(I)=0.5*(R1(I)+R1(I+1))
      DR2(1)=2.*(R2(1)-R1(1))
      DR2(M)=2.*(R1(M)-R2(M1))
      DO 40 I=2,M1
   40 DR2(I)=R2(I)-R2(I-1)
C     MAX=MAXMAG(DR1)
C     DRMAX=DR1(MAX)
C
C                DEFINE ALL DZ'S
C
      DO 100 J=1,N
  100 Z1(J)=(J-1)*200.E2
      DO 110 J=1,N1
  110 DZ1(J)=Z1(J+1)-Z1(J)
      DZ2(1)=2.*(0.5*(Z1(1)+Z1(1)))
      Z2(1)=0.5*DZ2(1)
      DO 120 J=2,N1
      DZ2(J)=0.5*(DZ1(J)+DZ1(J-1))
  120 Z2(J)=Z2(J-1)+DZ2(J)
      DZ2(N)=2.*(Z1(N)-Z1(N-1)-0.5*DZ1(N1))
C     MAX=MAXMAG(DZ1)
C     DZMAX=DZ1(MAX)
C
C                DEFINE CONSTANTS FOR SEVP SOLVER
C
      AX(1)=0.
      CX(MP)=0.
      AY(1)=0.
      CY(NP)=0.
      DO 50 I=1,M1
      AX(I+1)=R1(I)/(0.5*(R1(I)+R1(I+1))*DR1(I)*DR2(I))
   50 CX(I+1)=R1(I+1)/(0.5*(R1(I)+R1(I+1))*DR1(I)*DR2(I+1))
      DO 60 J=1,N1
      AY(J+1)=1./(DZ1(J)*DZ2(J))
   60 CY(J+1)=1./(DZ1(J)*DZ2(J+1))
      DO 70 J=1,NP
      DO 70 I=1,MP
   70 BB(I,J)=-CX(I)-AX(I)-CY(J)-AY(J)
      NSIZE=N1/NBLK+MOD(N1,2)
      DO 80 NB=1,NBLK1
   80 NBSIZ2(NB)=NSIZE
      NBSIZ2(NBLK)=N1-(NBLK-1)*NSIZE+NBLK1
```

*** MEMBER INIT

```
C
C                        A AND B ARE CONSTANT USED IN SUBROUTINE BOUNDV
C                        FOR CONSTANT DIV. AND VERT. CONDITIONS
C
      BNDA=R1(M1)/R1(M)
      BNDB=(R1(M1)+R1(M))*DR1(M1)/((R1(M1)+R1(M2))*R1(M)*DR1(M2))
      BNDB=0.
C
C                        DEFINE DENSITY RELATED CONSTANTS
C
      RHO=1.
      DO 130 J=1,N
  130 BV2(J)=1.E-6
      TBV=0.
      DO 135 J=1,N
  135 TBV=AMAX1(TBV,BV2(J))
      TBV=1./SQRT(TBV)
C
C                        DEFINE HORIZONTAL AND VERTICAL DIFFUSION COEFFIENTS
C
      COEFH=0.002*DR1(1)**2/DELT
      COEFZ=0.001*DZ1(1)**2/DELT
      DO 140 I=1,M1
  140 HK(I)=COEFH*(1.+5.*EXP(-FLOAT(M1-I)/7.))
      DO 150 J=1,N1
  150 ZK(J)=COEFZ*(1.+5.*(EXP(-FLOAT(J-1)/5.)+EXP(-FLOAT(N1-J)/5.)))
      RETURN
      END
```

CARD IMAGE FILE EDITOR(CIFEM) -- VERSION 05.29 DATE=10/26/82   TIME=14:12:12:99

*** MEMBER START

```
      SUBROUTINE START
      PARAMETER M=21,N=21
      PARAMETER M1=M-1,M2=M-2,N1=N-1,N2=N-2
      COMMON/ONE/VR1(M,N1),VT1(M,N1),VZ1(M1,N),B1(M1,N1),VR2(M,N1),
     1          VT2(M,N1),VZ2(M1,N),B2(M1,N1),VR3(M,N1),VT3(M,N1),
     2          VZ3(M1,N),B3(M1,N1),P(M1,N1)
      COMMON/TWO/R1(M),R2(M1),DR1(M1),DR2(M),Z1(N),Z2(N1),DZ1(N1),DZ2(N)
      COMMON/THR/RHO,RHOR(N1),RV2(N),ALPHA,BNCA,BNDB,CORI,G,RK(M),ZK(N)
      PARAMETER ND=2*M*N1+M1*N+M1*N1
      DIMENSION DATA1(ND),DATA2(ND)
      EQUIVALENCE (DATA1,VR1),(DATA2,VR2)
C
C                    INITIALIZE MASS FIELDS FOR A THEORETICAL RING
C
      I11=1
      I12=13
      I21=I12+1
      I22=M1
      BMAG=0.0002
      DO 10 I=I11,I12
   10 B1(I,N1)=BMAG*COS(FLOAT(I-I11)/8.*3.14159)*G/RHO
      DO 30 I=I21,I22
   30 B1(I,N1)=B1(I12,N1)*EXP(-FLOAT(I-I21+1)/4.)
      DO 40 J=1,N2
      FACT=EXP(FLOAT(J-N1)/5.)
      DO 40 I=1,M1
   40 B1(I,J)=B1(I,N1)*FACT
C
C                    PRESSURE IS OBTAINED HYDROSTATICALLY FROM BUOYANCY
C
      DO 50 I=1,M1
   50 P(I,1)=-0.5*RHO*DZ2(1)*B1(I,1)
      DO 60 J=2,N1
      DO 60 I=1,M1
   60 P(I,J)=P(I,J-1)-0.5*RHO*DZ2(J)*(B1(I,J)+B1(I,J-1))
C
C                    TANGENTIAL VELOCITY IS IN GRADIENT BALANCE WITH MASS
C
      DO 70 J=1,N1
      DO 70 I=2,M1
      PGF=(P(I,J)-P(I-1,J))/(RHO*DR2(I))
      RAD=(0.5*CORI*R1(I))**2+R1(I)*PGF
      JJ=J
      II=I
      IF(RAD.LT.0.)GO TO 100
   70 VT1(I,J)=-0.5*CORI*R1(I)+SQRT(RAD)
C
C                    SET DATA2=DATA1 FOR LEAPFROG
C
      DO 80 I=1,ND
   80 DATA2(I)=DATA1(I)
      CALL BOUNDV
      DO 90 I=1,ND
   90 DATA1(I)=DATA2(I)
      RETURN
  100 PRINT 110,II,JJ,PGF,RAD
  110 FORMAT(' RADICAL IN SUBROUTINE START IS NEGATIVE AT (I,J)=',2I5,
     1' PGF, RAD =',1P2E12.3)
      STOP
      END
```

CARD IMAGE FILE EDITOR(CIFER) -- VERSION 05.29 DATE=10/26/82 TIME=14:12:12:99

*** MEMBER BOUNDV

```
      SUBROUTINE BOUNDV
      PARAMETER M=21,N=21
      PARAMETER M1=M-1,M2=M-2,N1=N-1,N2=N-2
      COMMON/ONE/VR1(M,N1),VT1(M,N1),VZ1(M1,N),R1(M1,N1),VR2(M,N1),
     1           VT2(M,N1),VZ2(M1,N),R2(M1,N1),VR3(M,N1),VT3(M,N1),
     2           VZ3(M1,N),B3(M1,N1),P(M1,N1)
      COMMON/TWO/R1(M),R2(M1),DR1(M1),DR2(M),Z1(N),Z2(N1),DZ1(N1),DZ2(N)
      COMMON/THR/RHO,RHOR(N1),BVZ(N),ALPHA,BNDA,BNDB,CORI,G,HK(M),ZK(N)
C
C                 LATERAL BOUNDARY FOR TANGENTIAL AND RADIAL VELOCITIES
C                 ASSUMING CONTINUOUS VORTICITY AND DIVERGENCE
C
      DO 10 J=1,N1
      VR2(M,J)=BNDA*VR2(M1,J)+BNDB*(R1(M1)*VR2(M1,J)-R1(M2)*VR2(M2,J))
   10 VT2(M,J)=BNDA*VT2(M1,J)+BNDB*(R1(M1)*VT2(M1,J)-R1(M2)*VT2(M2,J))
      RETURN
      END
```

CARD IMAGE FILE EDITOR(CIFEM) -- VERSION 05.29 DATE=10/26/82 TIME=14:12:12:99

*** MEMBER DIFF

```
      SUBROUTINE DIFF
C
C                   COMPLETE THE DIFFUSION TERMS
C
      PARAMETER M=21,N=21
      PARAMETER M1=M-1,M2=M-2,N1=N-1,N2=N-2
      COMMON/ONE/VR1(M,N1),VT1(M,N1),VZ1(M1,N),B1(M1,N1),VR2(M,N1),
     1           VT2(M,N1),VZ2(M1,N),B2(M1,N1),VR3(M,N1),VT3(M,N1),
     2           VZ3(M1,N),B3(M1,N1),P(M1,N1)
      COMMON/TWO/R1(M),R2(M1),DR1(M1),DR2(M),Z1(N),Z2(N1),DZ1(N1),DZ2(N)
      COMMON/THR/RHO,RHOR(N1),BV2(N),ALPHA,BNDA,BNDB,CORI,G,HK(M),ZK(N)
      DIMENSION VR(M,N1),VT(M,N1),VZ(M1,N),B(M1,N1)
      EQUIVALENCE (VR,VR1),(VT,VT1),(VZ,VZ1),(B,B1)
C
C                   HORIZONTAL DIFFUSION OF RADIAL VELOCITY
C
      DO 10 J=1,N1
      DO 10 I=2,M1
   10 VR3(I,J)=VR3(I,J)+HK(I)*(((VR(I+1,J)-VR(I,J))/DR1(I)
     1          -(VR(I,J)-VR(I-1,J))/DR1(I-1))/DR2(I)-VR(I,J)/(R1(I)*R1(I))
     2          +0.5*((VR(I+1,J)-VR(I,J))/(DR1(I)*R2(I))
     3          +(VR(I,J)-VR(I-1,J))/(DR1(I-1)*R2(I-1))))
C
C                   HORIZONTAL DIFFUSION OF TANGENTIAL VELOCITY
C
      DO 20 J=1,N1
      DO 20 I=2,M1
   20 VT3(I,J)=VT3(I,J)+HK(I)*(((VT(I+1,J)-VT(I,J))/DR1(I)
     1          -(VT(I,J)-VT(I-1,J))/DR1(I-1))/DR2(I)-VT(I,J)/(R1(I)*R1(I))
     2          +0.5*((VT(I+1,J)-VT(I,J))/(DR1(I)*R2(I))
     3          +(VT(I,J)-VT(I-1,J))/(DR1(I-1)*R2(I-1))))
C
C                   HORIZONTAL DIFFUSION OF VERTICAL VELOCITY
C
      DO 30 J=2,N1
      DO 30 I=2,M2
   30 VZ3(I,J)=VZ3(I,J)+HK(I)*(((VZ(I+1,J)-VZ(I,J))/DR2(I+1)
     1          -(VZ(I,J)-VZ(I-1,J))/DR2(I))/DR1(I)
     2          +0.5*((VZ(I+1,J)-VZ(I,J))/(DR2(I+1)*R1(I+1))
     3          +(VZ(I,J)-VZ(I-1,J))/(DR2(I)*R1(I))))
      DO 40 J=2,N1
   40 VZ3(1,J)=VZ3(1,J)+HK(1)*((VZ(2,J)-VZ(1,J))/(DR2(1)*DR1(1))
     1          +0.5*(VZ(2,J)-VZ(1,J))/(DR2(2)*R1(2)))
      DO 50 J=2,N1
   50 VZ3(M1,J)=VZ3(M1,J)+HK(M1)*((-VZ(M1,J)+VZ(M2,J))/(DR2(M1)*DR1(M1))
     1          +(-VZ(M1,J)+VZ(M2,J))/(DR2(M1)*R1(M1)))
C
C                   HORIZONTAL DIFFUSION OF B
C
      DO 60 J=1,N1
      DO 60 I=2,M2
   60 B3(I,J)=B3(I,J)+HK(I)*(((B(I+1,J)-B(I,J))/DR2(I+1)
     1          -(B(I,J)-B(I-1,J))/DR2(I))/DR1(I)
     2          +0%5*((B(I+1,J)-B(I,J))/(DR2(I+1)*R1(I+1))
     3          +(B(I,J)-B(I-1,J))/(DR2(I)*R1(I))))
      DO 70 J=1,N1
   70 B3(1,J)=B3(1,J)+HK(1)*((B(2,J)-B(1,J))/(DR2(2)*DR1(1))
     1          +0.5*(B(2,J)-B(1,J))/(DR2(2)*R1(2)))
      DO 80 J=1,N1
   80 B3(M1,J)=B3(M1,J)+HK(M1)*((-B(M1,J)+B(M2,J))/(DR2(M1)*DR1(M1))
     1          -(B(M1,J)-B(M2,J))/(DR2(M1)*R1(M1)))
C
C                   VERTICAL DIFFUSION OF RADIAL VELOCITY
C
      DO 90 J=2,N2
      DO 90 I=2,M1
   90 VR3(I,J)=VR3(I,J)+ZK(J)*((VR(I,J+1)-VR(I,J))/DZ2(J+1)
     1          -(VR(I,J)-VR(I,J-1))/DZ2(J))/DZ1(J)
      DO 100 I=2,M1
  100 VR3(I,1)=VR3(I,1)+ZK(1)*(VR(I,2)-VR(I,1))/(DZ2(2)*DZ1(1))
      DO 110 I=2,M1
  110 VR3(I,N1)=VR3(I,N1)+ZK(N1)*(-VR(I,N1)+VR(I,N2))/(DZ2(N1)*DZ1(N1))
C
C                   VERTICAL DIFFUSION OF TANGENTIAL VELOCITY
C
```

```
      DO 120 J=2,N2
      DO 120 I=2,M1
  120 VT3(I,J)=VT3(I,J)+ZK(J)*((VT(I,J+1)-VT(I,J))/DZ2(J+1)
     1          -(VT(I,J)-VT(I,J-1))/DZ2(J))/DZ1(J)
      DO 130 I=2,M1
  130 VT3(I,1)=VT3(I,1)+ZK(1)*(VT(I,2)-VT(I,1))/(DZ2(2)*DZ1(1))
      DO 140 I=2,M1
  140 VT3(I,N1)=VT3(I,N1)+ZK(N1)*(-VT(I,N1)+VT(I,N2))/(DZ2(N1)*DZ1(N1))

C
C                    VERTICAL DIFFUSION OF VERTICAL VELOCITY
C
      DO 150 J=2,N1
      DO 150 I=1,M1
  150 VZ3(I,J)=VZ3(I,J)+ZK(J)*((VZ(I,J+1)-VZ(I,J))/DZ1(J)
     1          -(VZ(I,J)-VZ(I,J-1))/DZ1(J-1))/DZ2(J)
C
C                    VERTICAL DIFFUSION OF B
C
      DO 160 J=2,N2
      DO 160 I=1,M1
  160 B3(I,J)=B3(I,J)+ZK(J)*((B(I,J+1)-B(I,J))/DZ2(J+1)
     1          -(B(I,J)-B(I,J-1))/DZ2(J))/DZ1(J)
      DO 170 I=1,M1
  170 B3(I,1)=B3(I,1)+ZK(1)*(B(I,2)-B(I,1))/(DZ2(2)*DZ1(1))
      DO 180 I=1,M1
  180 B3(I,N1)=B3(I,N1)+ZK(N1)*(-B(I,N1)+B(I,N2))/(DZ2(N1)*DZ1(N1))
      RETURN
      END
```

```
CARD IMAGE FILE EDITOR(CIFEM) -- VERSION 05.29  DATE=10/26/82       TIME=14:12:12:99

*** MEMBER FRWRD

      SUBROUTINE FRWRD
      PARAMETER M=21,N=21
      PARAMETER M1=M-1,M2=M-2,N1=N-1,N2=N-2
      PARAMETER ND=2*M*N1+M1*N+M1*N1
      COMMON/ONE/DATA1(ND),DATA2(ND),DATA3(ND),P(M1,N1)
      COMMON/TWO/RHO,RHOR(N1),BV2(N),ALPHA,BNDA,BNDB,CORI,G,HK(M),ZK(N)
      COMMON/FOR/DELT,XTIME,ITIME,ISTEP,ISMO,ITAPE,TBV
C
C                   REPLACE DATA3 WITH THE NEW VALUES
C
      DO 10 I=1,ND
   10 DATA3(I)=DATA1(I)+2.*DELT*DATA3(I)
C
C                   TIME SMOOTHING
C
      IF(MOD(ISTEP,ISMO).NE.0)GO TO 30
      DO 20 I=1,ND
   20 DATA2(I)=DATA2(I)+(DATA1(I)+DATA3(I)-2.*DATA2(I))*ALPHA
   30 CONTINUE
C
C                   FORWARD MARCHING
C
      DO 40 I=1,ND
   40 DATA1(I)=DATA2(I)
      DO 50 I=1,ND
   50 DATA2(I)=DATA3(I)
C
C                   ZERO OUT DATA3 FOR NEXT STEP
C
      DO 60 I=1,ND
   60 DATA3(I)=0.
      RETURN
      END
```

CARD IMAGE FILE EDITOR(CIFER) -- VERSION 05.29 DATE=10/26/82 TIME=14:12:12:09

*** MEMBER CHECK

```
      SUBROUTINE CHECK
      PARAMETER M=21,N=21
      PARAMETER M1=M-1,M2=M-2,N1=N-1,N2=N-2
      COMMON/ONE/VR1(M,N1),VT1(M,N1),VZ1(M1,N),R1(M1,N1),VR2(M,N1),
     1           VT2(M,N1),VZ2(M1,N),R2(M1,N1),VR3(M,N1),VT3(M,N1),
     2           VZ3(M1,N),R3(M1,N1),P(M1,N1)
      COMMON/TWO/R1(M),R2(M1),DR1(M1),DR2(M),Z1(N),Z2(N1),DZ1(N1),DZ2(N)
      COMMON/FOR/DELT,XTIME,ITIME,ISTEP,ISMO,ITAPE,TBV
      DIMENSION WORK1(M),WORK2(N)
      DO 10 J=1,N1
      DO 20 I=1,M
   20 WORK1(I)=DR2(I)/AMAX1(1.,VR2(I,J))
      MIN=MINMAG(WORK1)+1
      DT=WORK1(MIN)*0.9
      DT=AMIN1(DT,DELT)
   10 CONTINUE
      DO 40 I=1,M1
      DO 30 J=1,N
   30 WORK2(J)=DZ2(J)/AMAX1(1.,VZ2(I,J))
      MIN=MINMAG(WORK2)+1
      DT=WORK2(MIN)*0.9
      DT=AMIN1(DT,DELT)
   40 CONTINUE
      DT=AMIN1(DT,TBV)
      IF(DT.GE.DELT)RETURN
      DELT=0.75*DELT
      PRINT 100,DELT
  100 FORMAT(//////,'*******DELT IS CHANGED TO',1PE11.2,' S*********')
      RETURN
      END
```

```
CARD IMAGE FILE EDITOR(CIFER) -- VERSION 05.29  DATE=10/26/82          TIME=14:12:12:99

*** MEMBER ZILCH
                                                                                0001000
      SUBROUTINE ZILCH(A,N)                                                     0002000
      DIMENSION A(N)                                                            0003000
      DO 10 I=1,N                                                               0004000
   10 A(I)=0.                                                                   0005000
      RETURN                                                                    0006000
      END
```

```
CARD IMAGE FILE EDITOR(CIFER) -- VERSION 05.29  DATE=10/26/82       TIME=14:12:12:09

*** MEMBER ADVECT

      SUBROUTINE ADVECT
C
C                    COMPUTE THE ADVECTIVE TERMS
C
      PARAMETER M=21,N=21
      PARAMETER M1=M-1,M2=M-2,N1=N-1,N2=N-2
      COMMON/ONE/VR1(M,N1),VT1(M,N1),VZ1(M1,N),B1(M1,N1),VR2(M,N1),
     1           VT2(M,N1),VZ2(M1,N),B2(M1,N1),VR3(M,N1),VT3(M,N1),
     2           VZ3(M1,N),B3(M1,N1),P(M1,N1)
      COMMON/TWO/R1(M),R2(M1),DR1(M1),DR2(M),Z1(N),Z2(N1),DZ1(N1),DZ2(N)
      COMMON/THR/RHO,RHOR(N1),BV2(N),ALPHA,BNDA,BNDB,CORI,G,RK(M),ZK(N)
      DIMENSION VR(M,N1),VT(M,N1),VZ(M1,N),B(M1,N1)
      EQUIVALENCE (VR,VR2),(VT,VT2),(VZ,VZ2),(B,B2)
C
C                    HORIZONTAL ADVECTION FOR RADIAL VELOCITY
C
      DO 10 J=1,N1
      DO 10 I=2,M1
   10 VR3(I,J)=-0.25*((VR(I,J)+VR(I-1,J))*(VR(I,J)-VR(I-1,J))/DR1(I-1)
     1           +(VR(I+1,J)+VR(I,J))*(VR(I+1,J)-VR(I,J))/DR1(I))
     2           +VR3(I,J)
C
C                    HORIZONTAL ADVECTION FOR TANGENTIAL VELOCITY
C
      DO 20 J=1,N1
      DO 20 I=2,M1
   20 VT3(I,J)=-0.25*((VR(I,J)+VR(I-1,J))*(VT(I,J)-VT(I-1,J))/DR1(I-1)
     1           +(VR(I+1,J)+VR(I,J))*(VT(I+1,J)-VT(I,J))/DR1(I))
     2           +VT3(I,J)
C
C                    HORIZONTAL ADVECTION FOR VERTICAL VELOCITY
C
      DO 30 J=2,N1
      DO 30 I=2,M2
   30 VZ3(I,J)=-0.25*((VR(I,J)+VR(I,J-1))*(VZ(I,J)-VZ(I-1,J))/DR2(I)
     1           +(VR(I+1,J)+VR(I+1,J-1))*(VZ(I+1,J)-VZ(I,J))/DR2(I+1))
     2           +VZ3(I,J)
      DO 40 J=2,N1
   40 VZ3(1,J)=-0.25*(VR(2,J)+VR(2,J-1))*(VZ(2,J)-VZ(1,J))/DR2(2)
     1           +VZ3(1,J)
      DO 50 J=2,N1
   50 VZ3(M1,J)=-0.25*(VR(M1,J)+VR(M1,J-1))*(VZ(M1,J)-VZ(M2,J))/DR2(M1)
     1           +VZ3(M1,J)
C
C                    HORIZONTAL ADVECTION FOR BUOYANCY
C
      DO 60 J=1,N1
      DO 60 I=2,M2
   60 B3(I,J)=B3(I,J)-0.5*(VR(I,J)*(B(I,J)-B(I-1,J))/DR2(I)
     1           +VR(I+1,J)*(B(I+1,J)-B(I,J))/DR2(I+1))
      DO 70 J=1,N1
   70 B3(1,J)=B3(1,J)-0.5*VR(2,J)*(B(2,J)-B(1,J))/DR2(2)
      DO 80 J=1,N1
   80 B3(M1,J)=B3(M1,J)-0.5*VR(M1,J)*(B(M1,J)-B(M2,J))/DR2(M1)
C
C                  . VERTICAL ADVECTION FOR RADIAL VELOCITY
C
      DO 90 J=2,N2
      DO 90 I=2,M1
   90 VR3(I,J)=VR3(I,J)-0.25*((VZ(I-1,J)+VZ(I,J))*(VR(I,J)-VR(I,J-1))
     1           /DZ2(J)+(VZ(I,J+1)+VZ(I-1,J+1))*(VR(I,J+1)-VR(I,J))
     2           /DZ2(J+1))
      DO 95 I=2,M1
   95 VR3(I,1)=VR3(I,1)-0.25*(VZ(I,2)+VZ(I-1,2))*(VR(I,2)-VR(I,1))
     1           /DZ2(2)
      DO 96 I=2,M1
   96 VR3(I,N1)=VR3(I,N1)-0.25*(VZ(I-1,N1)+VZ(I,N1))*(VR(I,N1)-VR(I,N2))
     1           /DZ2(N1)
C
C                    VERTICAL ADVECTION FOR TANGENTIAL VELOCITY
C
```

CARD IMAGE FILE EDITOR(CIFEN) -- VERSION 05.29 DATE=10/26/82   TIME=14:12:12:99

*** MEMBER ADVECT

```
      DO 100 J=2,N2
      DO 100 I=2,M1
  100 VT3(I,J)=VT3(I,J)-0.25*((VZ(I-1,J)+VZ(I,J))*(VT(I,J)-VT(I,J-1))
     1            /DZ2(J)+(VZ(I,J+1)+VZ(I-1,J+1))*(VT(I,J+1)-VT(I,J))
     2            /DZ2(J+1))
      DO 105 I=2,M1
  105 VT3(I,1)=VT3(I,1)-0.25*(VZ(I,2)+VZ(I-1,2))*(VT(I,2)-VT(I,1))
     1            /DZ2(2)
      DO 106 I=2,M1
  106 VT3(I,N1)=VT3(I,N1)-0.25*(VZ(I,N1)+VZ(I-1,N1))*(VT(I,N1)-VT(I,N2))
     1            /DZ2(N1)
C
C                     VERTICAL ADVECTION FOR VERTICAL VELOCITY
C
      DO 140 J=2,N1
      DO 140 I=1,M1
  140 VZ3(I,J)=VZ3(I,J)-0.25*((VZ(I,J-1)+VZ(I,J))*(VZ(I,J)-VZ(I,J-1))
     1            /DZ1(J-1)+(VZ(I,J+1)+VZ(I,J))*(VZ(I,J+1)-VZ(I,J))
     2            /DZ1(J))
C
C                     VERTICAL ADVECTION FOR B
C
      DO 150 J=2,N2
      DO 150 I=1,M1
  150 B3(I,J)=B3(I,J)-0.5*(VZ(I,J)*(B(I,J)-B(I,J-1))/DZ2(J)
     1          +VZ(I,J+1)*(B(I,J+1)-B(I,J))/DZ2(J+1))
      DO 160 I=1,M1
  160 B3(I,1)=B3(I,1)-0.5*VZ(I,2)*(B2(I,2)-B2(I,1))/DZ2(2)
      DO 170 I=1,M1
  170 B3(I,N1)=B3(I,N1)-0.5*VZ(I,N1)*(B(I,N1)-B(I,N2))/DZ2(N1)
C
C                     INERTIA TERMS FOR HORIZONTAL MOMENTUM
C
      DO 110 J=1,N1
      DO 110 I=2,M1
      VR3(I,J)=VR3(I,J)+VT(I,J)*(VT(I,J)/R1(I)+CORI)
  110 VT3(I,J)=VT3(I,J)-VR(I,J)*(VT(I,J)/R1(I)+CORI)
C
C                     BUOYANCY TERM FOR VERTICAL ACCELERATION
C
      DO 120 J=2,N1
      DO 120 I=1,M1
  120 VZ3(I,J)=VZ3(I,J)-0.5*(B(I,J)+B(I,J-1))
C
C                     STRATIFICATION TERM
C
      DO 130 J=1,N1
      DO 130 I=1,M1
  130 B3(I,J)=B3(I,J)+0.5*(VZ(I,J)*BV2(J)+VZ(I,J+1)*BV2(J+1))
      RETURN
      END
```

*** MEMBER ADVECT   ADDED TO   SOURCE -- 122 RECORDS

CARD IMAGE FILE EDITOR(CIFER) -- VERSION 05.29 DATE=10/26/82   TIME=14:12:12:09

*** MEMBER PLTOUT

```
      SUBROUTINE PLTOUT
      PARAMETER M=21,N=21
      PARAMETER M1=M-1,M2=M-2,N1=N-1,N2=N-2
      COMMON/ONE/VR1(M,N1),VT1(M,N1),VZ1(M1,N),B1(M1,N1),VR2(M,N1),
     1           VT2(M,N1),VZ2(M1,N),B2(M1,N1),VR3(M,N1),VT3(M,N1),
     2           VZ3(M1,N),B3(M1,N1),P(M1,N1)
      COMMON/TWO/R1(M),R2(M1),DR1(M1),DR2(M),Z1(N),Z2(N1),DZ1(N1),DZ2(N)
      COMMON/THR/RHO,RHOR(N1),BV2(N),ALPHA,ENDA,BNDB,CORI,G,RK(M),ZK(N)
      COMMON/FOR/DELT,XTIME,ITIME,ISTEP,ISMO,ITAPE,TBV
C
C                   THIS SUBROUTINE PRINT OUT FIELDS FOR A QUICK LOOK
C
      DIMENSION IDUM(M,N)
  700 FORMAT(/////,'  RADIAL VELOCITY (CM/S) AT T=',I6,' M')
  705 FORMAT(/////,'  TANGENTIAL VELOCITY (CM/S) AT T=',I6,' M')
  710 FORMAT(/////,'  VERTICAL VELOCITY (CM/S) AT T=',I6,' M')
  715 FORMAT(/////,'  BUOYANCY FIELD (*.001) AT T=',I6,' M')
  725 FORMAT(/////,'  PRESSURE (*10 DYNE/CM**2) AT TIME=',I6,' M')
  720 FORMAT(1H1,////,20X,'**********   OUTPUT AT TIME =',I6,' M    OR',
     1 F8.2,' DAY      ISTEP =',I7,'    *************')
      DAY=XTIME/86400.+0.0001
      PRINT 720,ITIME,DAY,ISTEP
      DO 10 J=1,N1
      DO 10 I=1,M
   10 IDUM(I,J)=VR2(I,J)
      PRINT 700,ITIME
      CALL MAP(IDUM,R1,Z2,M,N1)
      DO 20 J=1,N1
      DO 20 I=1,M
   20 IDUM(I,J)=VT2(I,J)
      PRINT 705,ITIME
      CALL MAP(IDUM,R1,Z2,M,N1)
      DO 30 J=1,N
      DO 30 I=1,M1
   30 IDUM(I,J)=VZ2(I,J)
      PRINT 710,ITIME
      CALL MAP(IDUM,R2,Z1,M1,N)
      DO 40 J=1,N1
      DO 40 I=1,M1
   40 IDUM(I,J)=B2(I,J)*1.E3
      PRINT 715,ITIME
      CALL MAP(IDUM,R2,Z2,M1,N1)
      DO 50 J=1,N1
      DO 50 I=1,M1
   50 IDUM(I,J)=P(I,J)*1.E-1
      PRINT 725,ITIME
      CALL MAP(IDUM,R2,Z2,M1,N1)
      RETURN
      END
```

CARD IMAGE FILE EDITOR(CIPEN) -- VERSION 05.29 DATE=10/26/82   TIME=14:12:12:09

*** MEMBER MAP

```
      SUBROUTINE MAP(A,R,Z,MM,NN)
      PARAMETER M=21,N=21
      DIMENSION R(MM),Z(NN)
      INTEGER A (M,N),IR(M),IZ(N)
   70 FORMAT(1H ,7X,25I5)
   80 FORMAT(1H ,I4,3X,25I5)
      MP=MIN0(25,MM)
      DO 10 I=1,MP
   10 IR(I)=R(I)*1.E+5+0.1
      DO 20 J=1,NN
   20 IZ(J)=Z(J)*1.E+6+0.1
      PRINT 70
      PRINT 70,(IR(I),I=1,MP)
      PRINT 70
      DO 30 JJ=1,NN
      J=NN+1-JJ
   30 PRINT 80,IZ(J),(A(I,J),I=1,MP)
      RETURN
      END
```

*** MEMBER PRESS

```
      SUBROUTINE PRESS
C
C                   THIS SUBROUTINE SETS UP FORCING FUNCTIONS AND BOUNDARY
C                   CONDITIONS FOR THE PRESSURE DIAGNOSTIC EQUATIONS FOR S
C
      PARAMETER M=21,N=21
      PARAMETER M1=M-1,M2=M-2,N1=N-1,N2=N-2
      PARAMETER NBLK=2,NBLK1=NBLK-1
      REAL*8 RCOR,RINV,RINV1,RTILDA,DUMMY1
      COMMON/ONE/VR1(M,N1),VT1(M,N1),VZ1(M1,N),B1(M1,N1),VR2(M,N1),
     1           VT2(M,N1),VZ2(M1,N),B2(M1,N1),VR3(M,N1),VT3(M,N1),
     2           VZ3(M1,N),B3(M1,N1),P(M1,N1)
      COMMON/TWO/R1(M),R2(M1),DR1(M1),DR2(M),Z1(N),Z2(N1),DZ1(N1),DZ2(N)
      COMMON/THR/RHO,RHOR(N1),BV2(N),ALPHA,BNDA,BNDR,CORI,G,HK(M),ZK(N)
C
C                     MP*NP IS THE SIZE OF X AND F
C                     MP=M1+2,NP=N1+NBLK+1
C
      PARAMETER MP=M+1,NP=N+1
      PARAMETER MP1=MP-1,MP2=MP-2,NP1=NP-1,NP2=NP-2
      COMMON/EVP/RINV(MP2,MP2,NBLK),RINV1(MP2,MP2,NBLK1),RCOR(MP,3),
     1           RTILDA(MP2),F(MP,NP),NBSIZ2(NBLK),IS(NBLK),SLMF(NBLK),
     2           IE(NBLK),F11(MP),F1N(MP),F21(NP),F2M(NP),AX(MP),AY(NP),
     3           PB(MP,NP),CX(MP),CY(NP)
      DIMENSION DUMMY1(MP2,MP2),X(MP,NP)
      EQUIVALENCE(DUMMY1,RINV(1,1,NBLK))
      PARAMETER MPNP=MP*NP
      DATA DUMMY1/MPNP*0./,X/MPNP*0./
      DATA NCALL/0/
C  NBSIZ2 REPRESENTS NUMBER OF INTERIOR GRID POINTS IN EACH BLOCK IN X-DI
C N2 REPRESENTS NUMBER OF INTERIOR GRID POINTS IN Y-DIRECTION
C NBLK REPRESENTS NUMBER OF BLOCKS IN X-DIRECTION
C THE VARIABLES A11,A1N,A21,A2M TAKES THE VALUE 0 FOR DIRICHLET B.C.
C  AND 1 FOR NEUMANN B.C.  AT THEIR RESPECTIVE BOUNDARIES  A11 CORRESPOND
C  J=1      A1N TO J=N          A21   TO I=1       A2M   TO I=M
C BOUNDARY CONDITIONS ARE
C   X(I,1)=(1-A11)*X(I,1)+A11*(X(I,2)-F11(I))
C     X(I,NP)=(1-A1N)*X(I,NP)+A1N*(X(I,NP-1)+F1N(I))
C   X(1,J)=(1-A21)*X(1,J)+A21*(X(2,J)-F21(J))
C     X(MP,J)=(1-A2M)*X(MP,J)+A2M*(X(MP-1,J)+F2M(J))
      NCALL=NCALL+1
C
C                     DEFINE THE FORCING FUNCTION OF THE ELLIPTIC EQUATION
C
      DO 10 J=1,NP2
      DO 10 I=1,MP2
   10 F(I+1,J+1)=(CX(I+1)*DR2(I+1)*VR3(I+1,J)+VZ3(I,J+1)/DZ1(J)
     1            -AX(I+1)*DR2(I)*VR3(I,J)-VZ3(I,J)/DZ1(J))*RHO
C
C                   SET UP AN INITIAL GUESS
C
```

```
CARD IMAGE FILE EDITOR(CIFER) -- VERSION 05.29  DATE=10/26/82       TIME=14:12:12:99

*** MEMBER PRESS

      IF(NCALL.GT.1)GO TO 30
      DO 20 J=1,NP2
      DO 20 I=1,MP2
   20 X(I+1,J+1)=P(I,J)
   30 CONTINUE
      CALL ZILCH(F11,MP)
      CALL ZILCH(F1N,MP)
      CALL ZILCH(F21,NP)
C
C                     DEFINE THE FORCING AT BOUNDARY SO THAT THERE
C                     IS GRADIENT BALANCE AT OUTER BOUNDARY
C
      DO 605 J=2,NP1
      F2M(J)=RHO*DR2(M)*VT2(M,J-1)*(VT2(M,J-1)/R1(M)+CORI)
  605 CONTINUE
      A11=1
      A1N=1
      A21=1
      A2M=1
      DO 101 J=2,NP1
      BB(2,J)=BB(2,J)+AX(2)*A21
      F(2,J)=F(2,J)+AX(2)*F21(J)*A21
      X(1,J)=(1.0-A21)*X(1,J)
      BB(MP-1,J)=BB(MP-1,J)+CX(MP-1)*A2M
      F(MP-1,J)=F(MP-1,J)-CX(MP-1)*F2M(J)*A2M
      X(MP,J)=(1.0-A2M)*X(MP,J)
  101 CONTINUE
      DO 102 I=2,MP1
      BB(I,2)=BB(I,2)+AY(2)*A11
      F(I,2)=F(I,2)+AY(2)*F11(I)*A11
      X(I,1)=(1.0-A11)*X(I,1)
      BB(I,NP-1)=BB(I,NP-1)+CY(NP-1)*A1N
      F(I,NP-1)=F(I,NP-1)-CY(NP-1)*F1N(I)*A1N
      X(I,NP)=(1.0-A11)*X(I,NP)
  102 CONTINUE
      IF(NCALL.EQ.1)CALL BSM1
      ERROR=1.E-3
      CALL BSM2(X,ERROR,A11,A1N,A21,A2M)
C
C                     DEFINE THE DIAGNOSED PRESSURE
C
      DO 110 J=1,N1
      DO 110 I=1,M1
  110 P(I,J)=X(I+1,J+1)
  115 CONTINUE
C
C                     ADD PRESSURE GRADIENT FORCES TO VR3 AND VZ3
C
      DO 120 J=1,N1
      DO 120 I=2,M1
  120 VR3(I,J)=VR3(I,J)-(P(I,J)-P(I-1,J))/(RHO*DR2(I))
      DO 130 J=2,N1
      DO 130 I=1,M1
  130 VZ3(I,J)=VZ3(I,J)-(P(I,J)-P(I,J-1))/(RHO*DZ2(J))
      RETURN
      END
```

*** MEMBER BSM1

```
      SUBROUTINE BSM1
      PARAMETER M=21,N=21
      PARAMETER M1=M-1,M2=M-2,N1=N-1,N2=N-2
      PARAMETER MP=M+1,NP=N+1
      PARAMETER MP1=MP-1,MP2=MP-2,NP1=NP-1,NP2=NP-2
      PARAMETER NBLK=2,NBLK1=NBLK-1
      REAL*8 RCOR,RINV,RINV1,RTILDA,DUMMY1
      COMMON/TMP/R1(M),R2(M1),DR1(M1),DR2(M),Z1(N),Z2(N1),DZ1(N1),DZ2(N)
      COMMON/EVP/RINV(MP2,MP2,NBLK),RINV1(MP2,MP2,NBLK1),RCOR(MP,3),
     1              RTILDA(MP2),F(MP,NP),NBSIZ2(NBLK),IS(NBLK),SLMP(NBLK),
     2              IE(NBLK),F11(MP),F1N(MP),F21(NP),F2M(NP),AX(MP),AY(NP),
     3              BB(MP,NP),CX(MP),CY(NP)
      DIMENSION DUMMY1(MP2,MP2)
      EQUIVALENCE (DUMMY1,RINV(1,1,NBLK))
      IE(1)=NBSIZ2(1)+2
      DO 90 NB=2,NBLK
      IE(NB)=IE(NB-1)+NBSIZ2(NB)+1
   90 CONTINUE
      DO 95 NB=1,NBLK1
      IS(NB+1)=IE(NB)-1
   95 CONTINUE
      IS(1)=1
      DO 115 I1=1,MP2
      DO 110 J=1,3
      DO 110 I=1,MP
      RCOR(I,J)=0.0
  110 CONTINUE
      RCOR(I1+1,2)=1.0
      NBS=IE(1)-1
      DO 130 J1=2,NBS
      DO 135 I=2,MP1
      RCOR(I,3)=(-AX(I)*RCOR(I-1,2)-AY(J1)*RCOR(I,1)-BB(I,J1)*
     1RCOR(I,2)-CX(I)*RCOR(I+1,2))/CY(J1)
  135 CONTINUE
      DO 140 I=1,MP
      RCOR(I,1)=RCOR(I,2)
      RCOR(I,2)=RCOR(I,3)
  140 CONTINUE
  130 CONTINUE
      DO 145 I=1,MP2
      RINV(I1,I,1)=RCOR(I+1,1)
      DUMMY1(I1,I)=RCOR(I+1,2)
  145 CONTINUE
  115 CONTINUE
      CALL MATINV(DUMMY1)
      DO 160 I=1,MP2
      DO 160 J=1,MP2
      RINV1(I,J,1)=0.0
      DO 161 K=1,MP2
      RINV1(I,J,1)=RINV1(I,J,1)+DUMMY1(I,K)*RINV(K,J,1)
  161 CONTINUE
  160 CONTINUE
      DO 170 I=1,MP2
      DO 170 J=1,MP2
      RINV(I,J,1)=DUMMY1(I,J)
  170 CONTINUE
      DO 205 NB=2,NBLK
      DO 215 I1=1,MP2
      DO 210 J=1,3
      DO 210 I=1,MP
      RCOR(I,J)=0.0
  210 CONTINUE
      DO 220 I=1,MP2
      RCOR(I+1,1)=RINV1(I1,I,NB-1)
  220 CONTINUE
      RCOR(I1+1,2)=1.0
      IE1=IE(NB-1)
      IE2=IE(NB)-1
      IF(NB.LT.NBLK) GO TO 232
      IE2=IE2-1
  232 CONTINUE
      DO 230 J1=IE1,IE2
      DO 235 I=2,MP1
      RCOR(I,3)=(-AX(I)*RCOR(I-1,2)-AY(J1)*RCOR(I,1)-BB(I,J1)*
     1RCOR(I,2)-CX(I)*RCOR(I+1,2))/CY(J1)
  235 CONTINUE
      DO 240 I=1,MP
```

CARD IMAGE FILE EDITOR(CIFER) -- VERSION 05.29 DATE=10/26/82 TIME=14:12:12:99

*** MEMBER BSM1

```
      RCOR(I,1)=RCOR(I,2)
      RCOR(I,2)=RCOR(I,3)
  240 CONTINUE
  241 CONTINUE
  230 CONTINUE
      IF(NB.EQ.NBLK) GO TO 246
      DO 245 I=1,MP2
      RINV(I1,I,NB)=RCOR(I+1,1)
  245 CONTINUE
      DO 247 I=1,MP2
      DUMMY1(I1,I)=RCOR(I+1,2)
  247 CONTINUE
      GO TO 249
  246 CONTINUE
      DO 248 I=2,MP1
      DUMMY1(I1,I-1)=AX(I)*RCOR(I-1,2)+AY(NP-1)*RCOR(I,1)+
     1BH(I,NP-1)*RCOR(I,2)+CX(I)*RCOR(I+1,2)
  248 CONTINUE
  249 CONTINUE
  215 CONTINUE
      CALL MATINV(DUMMY1)
      IF(NB.EQ.NBLK) GO TO 275
      DO 260 J=1,MP2
      DO 260 I=1,MP2
      RINV1(I,J,NB)=0.0
      DO 261 K=1,MP2
      RINV1(I,J,NB)=RINV1(I,J,NB)+DUMMY1(I,K)*RINV(K,J,NB)
  261 CONTINUE
  260 CONTINUE
      DO 270 J=1,MP2
      DO 270 I=1,MP2
      RINV(I,J,NB)=DUMMY1(I,J)
  270 CONTINUE
  275 CONTINUE
  295 CONTINUE
      RETURN
      END
```

CARD IMAGE FILE EDITOR(CIFED) -- VERSION 05.29 DATE=10/26/82 TIME=14:12:12:99

*** MEMBER MATINV

```
      SUBROUTINE MATINV(B)
      PARAMETER M=21
      PARAMETER MP=M+1
      REAL*8 B(MP,MP)
      REAL*8 B1(MP),B2(MP)
      MP1=MP-1
      DO 110 I=1,MP1
      B1(1)=1.0/B(I,I)
      B(I,I)=1.0
      DO 112 J=1,MP
      B(I,J)=B(I,J)*B1(1)
  112 CONTINUE
      IP1=I+1
      DO 120 I1=IP1,MP
      B1(I1)=B(I1,I)
  120 CONTINUE
      DO 125 I1=IP1,MP
      B(I1,I)=0.0
  125 CONTINUE
      DO 127 J=1,MP
      B2(J)=B(I,J)
  127 CONTINUE
      DO 135 I1=IP1,MP
      DO 135 J=1,MP
      B(I1,J)=B(I1,J)-B1(I1)*B2(J)
  135 CONTINUE
  110 CONTINUE
      B1(1)=1.0/B(MP,MP)
      B(MP,MP)=1.0
      DO 140 J=1,MP
      B(MP,J)=B(MP,J)*B1(1)
  140 CONTINUE
      DO 150 I=2,MP
      DO 155 I2=1,I
      B1(I2)=B(I2,I)
  155 CONTINUE
      IM1=I-1
      DO 156 I2=1,IM1
      B(I2,I)=0.0
  156 CONTINUE
      DO 157 J=1,MP
      B2(J)=B(I,J)
  157 CONTINUE
      IM1=I-1
      DO 160 I2=1,IM1
      DO 160 J=1,MP
      B(I2,J)=B(I2,J)-B1(I2)*B2(J)
  160 CONTINUE
  150 CONTINUE
      RETURN
      END
```

CARD IMAGE FILE EDITOR(CIFEM) -- VERSION 05.29 DATE=10/26/82   TIME=14:12:12:99

*** MEMBER BSM2

```
      SUBROUTINE BSM2(X,ERROR,A11,A1N,A21,A2M)
      PARAMETER M=21,N=21
      PARAMETER NBLK=2,NBLK1=NBLK-1
      PARAMETER MP=M+1,NP=N+1
      PARAMETER MP1=MP-1,MP2=MP-2,NP1=NP-1,NP2=NP-2
      REAL*8 RCOR,RINV,RINV1,RTILDA
      COMMON/EVP/RINV(MP2,MP2,NBLK),RINV1(MP2,MP2,NBLK1),RCOR(MP,3),
     1           RTILDA(MP2),F(MP,NP),NOSIZ2(NBLK),IS(NBLK),SUMF(NBLK),
     2           IE(NBLK),F11(MP),F1N(MP),F21(NP),F2M(NP),AX(MP),AY(NP),
     3           BB(MP,NP),CX(MP),CY(NP)
      DIMENSION X(MP,NP)
      DO 90 NB=1,NBLK
      SUMF(NB)=0.0
   90 CONTINUE
      DO 95 NB=1,NBLK
      DO 95 I=2,MP1
      SUMF(NB)=SUMF(NB)+ABS(F(I,IE(NB)-1))
   95 CONTINUE
      DO 96 NB=1,NBLK
      IF(SUMF(NB).GT.0.0) GO TO 96
      SUMF(NB)=1.0
   96 CONTINUE
      NSTART=1
      DO 199 IT3=1,5
      DO 200 NB=NSTART,NBLK
      ISP1=IS(NB)+1
      IEM2=IE(NB)-2
      DO 205 J=ISP1,IEM2
      DO 205 I=2,MP1
      X(I,J+1)=(F(I,J)-AX(I)*X(I-1,J)-AY(J)*X(I,J-1)-BB(I,J)*
     1X(I,J)-CX(I)*X(I+1,J))/CY(J)
  205 CONTINUE
      IF(NB.EQ.NBLK) GO TO 200
      DO 522 IT=1,10
      J1=IE(NB)-1
      DO 215 I=2,MP1
      RTILDA(I-1)=X(I,J1+1)-(F(I,J1)-AX(I)*X(I-1,J1)-AY(J1)*
     1X(I,J1-1)-BB(I,J1)*X(I,J1)         -CX(I)*X(I+1,J1))/CY(J1)
  215 CONTINUE
      A2=0.0
      DO 216 I=1,MP2
      A2=A2+DABS(RTILDA(I))
  216 CONTINUE
      A3=A2/SUMF(NB)
      IF(A3.LE.0.1) GO TO 230
      DO 217 J=1,3
      DO 217 I=1,MP
      RCOR(I,J)=0.0
  217 CONTINUE
      DO 223 J=1,MP2
      RCOR(J+1,2)=0.0
      DO 223 J1=1,MP2
      RCOR(J+1,2)=RCOR(J+1,2)+RTILDA(J1)*RINV(J1,J,NB)
  223 CONTINUE
      IF(NB.EQ.1) GO TO 251
      DO 225 J=2,MP1
      RCOR(J,1)=0.0
      DO 225 K=2,MP1
      RCOR(J,1)=RCOR(J,1)          +RCOR(K,2)*RINV1(K-1,J-1,NB-1)
  225 CONTINUE
      DO 226 I=2,MP1
      X(I,IS(NB))=X(I,IS(NB))+RCOR(I,1)
  226 CONTINUE
  251 CONTINUE
      CALL BSM3(X,IS(NB),IE(NB))
  522 CONTINUE
  230 CONTINUE
      J1=IE(NB)-1
      DO 220 I=2,MP1
      X(I,J1+1)=(F(I,J1)-AX(I)*X(I-1,J1)-AY(J1)*X(I,J1-1)-
     1BB(I,J1)*X(I,J1)-CX(I)*X(I+1,J1))/CY(J1)
  220 CONTINUE
  501 CONTINUE
  200 CONTINUE
      DO 300 NB1=1,NBLK
      NB=NBLK-NB1+1
      ISP1=IS(NB)+1
```

```
*** MEMBER BSM2
      IEM2=IE(NB)-2
      J=IEM2
      IF(NB.EQ.NBLK) GO TO 502
      DO 305 I=2,MP1
      X(I,J+1)=(F(I,J)-AX(I)*X(I-1,J)-AY(J)*X(I,J-1)-BB(I,J)*
     1X(I,J)-CX(I)*X(I+1,J))/CY(J)
  305 CONTINUE
  502 CONTINUE
      DO 552 IT=1,10
      IF(NB.EQ.NBLK) GO TO 317
      J1=IE(NB)-1
      DO 315 I=2,MP1
      RTILDA(I-1)=X(I,J1+1)-(F(I,J1)-AX(I)*X(I-1,J1)-AY(J1)*
     1X(I,J1-1)-BB(I,J1)*X(I,J1)-CX(I)*X(I+1,J1))/CY(J1)
  315 CONTINUE
      GO TO 318
  317 CONTINUE
      DO 319 I=2,MP1
      RTILDA(I-1)=F(I,NP-1)-(AX(I)*X(I-1,NP-1)+AY(NP-1)*X(I,NP-2)+
     1BB(I,NP-1)*X(I,NP-1)+CX(I)*X(I+1,NP-1))
  319 CONTINUE
  318 CONTINUE
      A2=0.0
      DO 316 I=1,MP2
      A2=A2+DABS(RTILLA(I    ))
  316 CONTINUE
      A3=A2/SUMF(NB)
      IF(A3.LE.ERROR) GO TO 300
      DO 320 J=1,3
      DO 320 I=1,MP
      RCOR(I,J)=0.0
  320 CONTINUE
      DO 324 J=1,MP2
      RCOR(J+1,2)=0.0
      DO 324 J1=1,MP2
      RCOR(J+1,2)=RCOR(J+1,2)+RTILDA(J1)*RINV(J1,J,NB)
  324 CONTINUE
      IF(NB.EQ.1) GO TO 551
      DO 325 J=2,MP1
      RCOR(J,1)=0.0
      DO 325 K=2,MP1
      RCOR(J,1)=RCOR(J,1)          +RCOR(K,2)*RINV1(K-1,J-1,NB-1)
  325 CONTINUE
      DO 326 I=2,MP1
      X(I,IS(NB))=X(I,IS(NB))+RCOR(I,1)
  326 CONTINUE
  551 CONTINUE
      CALL BSM3(X,IS(NB),IE(NB))
  552 CONTINUE
  300 CONTINUE
      J1=IE(1)
      DO 330 I=2,MP1
      RTILDA(I-1)=X(I,J1+1)-(F(I,J1)-AX(I)*X(I-1,J1)-AY(J1)*
     1X(I,J1-1)-BB(I,J1)*X(I,J1)          -CX(I)*X(I+1,J1))/CY(J1)
  330 CONTINUE
      A2=0.0
      DO 332 I=1,MP2
      A2=A2+DABS(RTILDA(I))
  332 CONTINUE
      A3=A2/SUMF(1)
      IF(A3.LE.ERROR) GO TO 201
      NSTART=2
  199 CONTINUE
  201 CONTINUE
      DO 350 J=2,MP1
      X(1,J)=(1.0-A21)*X(1,J)+A21*(X(2,J)-F21(J))
      X(MP,J)=(1.0-A2M)*X(MP,J)+A2M*(X(MP-1,J)+F2M(J))
  350 CONTINUE
      DO 360 I=2,NP1
      X(I,1)=(1.0-A11)*X(I,1)+A11*(X(I,2)-F11(I))
      X(I,NP)=(1.0-A1N)*X(I,NP)+A1N*(X(I,NP-1)+F1N(I))
  360 CONTINUE
      DO 371 J=2,MP1
      BB(2,J)=BB(2,J)-AX(2)*A21
      F(2,J)=F(2,J)-AX(2)*F21(J)*A21
      BB(MP-1,J)=BB(MP-1,J)-CX(MP-1)*A2M
```

AD-A137 421 TROPICAL WEATHER SYSTEM AND OCEAN MODELING(U) SCIENCE APPLICATIONS INC MCLEAN VA S CHANG 1983 SAI-83-1155 N00014-82-C-2306 2/2

UNCLASSIFIED F/G 4/2 NL

END

FILMED

DTIC

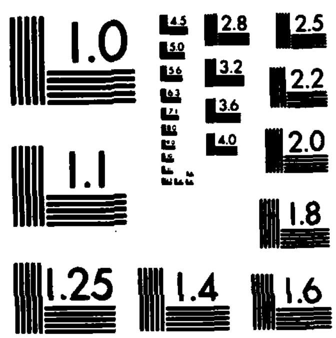

MICROCOPY RESOLUTION TEST CHART
NATIONAL BUREAU OF STANDARDS-1963-A

*** MEMBER MSM2

```
      F(MP-1,J)=F(MP-1,J)+CX(MP-1)*F2M(J)*A2M
  371 CONTINUE
      DO 372 I=2,MP1
      BB(I,2)=BB(I,2)-AY(2)*A11
      F(I,2)=F(I,2)-AY(2)*F11(I)*A11
      BB(I,NP-1)=BB(I,NP-1)-CY(NP-1)*A1N
      F(I,NP-1)=F(I,NP-1)+CY(NP-1)*F1N(I)*A1N
  372 CONTINUE
      RETURN
      END
```

CARD IMAGE FILE EDITOR(CIFED) -- VERSION 05.29 DATE=10/26/82 TIME=14:12:12:00

*** MEMBER BSM3

```
      SUBROUTINE BSM3(X,ISS,IEE)
      PARAMETER M=21,N=21
      PARAMETER NBLK=2,NBLK1=NBLK-1
      PARAMETER MP=M+1,NP=N+1
      PARAMETER MP1=MP-1,MP2=MP-2,NP1=NP-1,NP2=NP-2
      REAL*8 RCOR,RINV,RINV1,RTILDA
      DIMENSION X(MP,NP)
      COMMON/EVP/RINV(MP2,MP2,NBLK),RINV1(MP2,MP2,NBLK1),RCOR(MP,3),
     1           RTILDA(MP2),F(MP,NP),NBSIZ2(NBLK),IS(NBLK),SLMF(NBLK),
     2           IE(NBLK),F11(MP),F1N(MP),F21(NP),F2M(NP),AX(MP),AY(NP),
     3           BB(MP,NP),CX(MP),CY(NP)
      DO 135 I=2,MP1
      X(I,ISS+1)=X(I,ISS+1)+RCOR(I,2)
  135 CONTINUE
      ISP1=ISS+1
      IEM2=IEE-2
      DO 140 J=ISP1,IEM2
      DO 145 I=2,MP1
      RCOR(I,3)=(-AX(I)*RCOR(I-1,2)-AY(J)*RCOR(I,1)-BB(I,J)*
     1RCOR(I,2)-CX(I)*RCOR(I+1,2))/CY(J)
  145 CONTINUE
      DO 150 I=2,MP1
      X(I,J+1)=X(I,J+1)+RCOR(I,3)
      RCOR(I,1)=RCOR(I,2)
      RCOR(I,2)=RCOR(I,3)
  150 CONTINUE
  140 CONTINUE
      RETURN
      END
```

CARD IMAGE FILE EDITOR(CIFEM) -- VERSION 05.29 DATE=10/26/82   TIME=14:16:32:36

<<SPLIT OCEAN1,SOURC1,PRINT,SEQ

```
      PROGRAM OCEAN
      PARAMETER M=21,N=21
      PARAMETER M1=M-1,M2=M-2,N1=N-1,N2=N-2
      PARAMETER ND=2*M*N1+M1*N1
      DIMENSION DATA1(ND),DATA2(ND),DATA3(ND)
      COMMON/ONE/VR1(M,N1),VT1(M,N1),B1(M1,N1),VR2(M,N1),
     1          VT2(M,N1),B2(M1,N1),VR3(M,N1),VT3(M,N1),
     2          B3(M1,N1),P(M1,N1),VZ(M1,N)
      EQUIVALENCE (DATA1,VR1),(DATA2,VR2),(DATA3,VR3)
      DATA DATA1/ND*0./,DATA2/ND*0./,DATA3/ND*0./
      COMMON/TWO/R1(M),R2(M1),DR1(M1),DR2(M),Z1(N),Z2(N1),DZ1(N1),DZ2(N)
      COMMON/THR/RHO,RHOR(N1),BV2(N),ALPHA,BNOA,BNOB,CORI,G,HK(M),ZK(N)
      COMMON/FOR/DELT,XTIME,ITIME,ISTEP,ISNB,ITAPE,TBV
      CALL INDUMP
  100 FORMAT(I4)
      READ(5,100)ITIME
      READ(5,100)ITER
      READ(5,100)IOUT
      READ(5,100)ISNB
      ISTEP=0
      READ(5,100)ITAPE
      CALL INIT
      IF(ITIME.EQ.0)GO TO 10
C
C                 CONTINUED INTEGRATION FROM A HISTORY TAPE
C
      READ(1)ITIME,DATA1,DATA2,P
      GO TO 20
   10 CALL START
   20 XTIME=ITIME*3600.
C
C                 PRINT OUT INITIAL FIELDS
C
      CALL PUTOUT
      IF(ITER.EQ.0)STOP
      DO 90 ISTEP=1,ITER
C
C                 COMPUTE HYDROSTATIC PRESSURE AND DIAGNOSE VERTICAL VE
C
      CALL UP
C
C              COMPLTE ALL INVISCID TERMS
C
      CALL ADVECT
C
C                 COMPUTE VISCOUS TERMS
C
      CALL DIFF
C
C                 MARCHING IN TIME
C                 FIRST TIME STEP IS FORWARD IF START IS CALLED
C
      IF(ISTEP.EQ.1.AND.ITIME.EQ.0)DELT=0.5*DELT
      CALL FRWRD
      IF(ISTEP.EQ.1.AND.ITIME.EQ.0)DELT=2.*DELT
C
C                 DEFINE BOUNDARY VALUES FOR VELOCITY
C
      CALL BOUNDV
C
C                 CHECK IF DELT IS STABLE
CC
      CALL CHECK
      XTIME=XTIME+DELT
      ITIME=XTIME/3600.
C
C                 PRINT OUT RESULTS EVERY IOUT STEPS
C
      IF(MOD(ISTEP,IOUT).EQ.0)CALL PUTOUT
C
C                 WRITE HISTORY TAPE EVERY ITAPE STEPS
C
      IF(MOD(ISTEP,ITAPE).EQ.0)WRITE(2)ITIME,DATA1,DATA2,P
   90 CONTINUE
      STOP
      END
```

CARD IMAGE FILE EDITOR(CIFEM) -- VERSION 05.29   DATE=10/26/82   TIME=14:16:32:36

*** MEMBER INIT

```
      SUBROUTINE  INIT
      PARAMETER M=21,N=21
      PARAMETER M1=M-1,M2=M-2,N1=N-1,N2=N-2
      COMMON/ONE/VR1(M,N1),VT1(M,N1),B1(M1,N1),VR2(M,N1),
     1           VT2(M,N1),B2(M1,N1),VR3(M,N1),VT3(M,N1),
     2           B3(M1,N1),P(M1,N1),VZ(M1,N)
      COMMON/TWO/R1(M),R2(M1),DR1(M1),DR2(M),Z1(N),Z2(N1),DZ1(N1),DZ2(N)
      COMMON/THR/RHO,RHOR(N1),BV2(N),ALPHA,BNDA,BNDB,CORI,G,HK(M),ZK(N)
      COMMON/FOR/DELT,XTIME,ITIME,ISTEP,ISHO,ITAPE,TBV
C
C                     INITIALIZE ALL DEPENDENT VARIABLES AND CONSTANTS
C
C
C                      ALPHA IS THE NONDIMENSIONAL SMOOTHING COEF.
C                      FOR TIME SMOOTHING IN SUBROUTINE FRWRD
C
      DELT=900.
      ALPHA=0.10
      G=980.
      LAT=30
      CORI=2.*7.2722E-5*SIN(LAT*3.14159/180.)
C
C                      DEFINE RADII AT GRID POINTS AND ALL GRID INTERVALS
C
      DO 10 I=1,M1
   10 DR1(I)=20.E5
      R1(1)=0.
      DO 20 I=2,M
   20 R1(I)=R1(I-1)+DR1(I-1)
      DO 30 I=1,M1
   30 R2(I)=0.5*(R1(I)+R1(I+1))
      DR2(1)=2.*(R2(1)-R1(1))
      DR2(M)=2.*(R1(M)-R2(M1))
      DO 40 I=2,M1
   40 DR2(I)=R2(I)-R2(I-1)
C     MAX=MAXMAG(DR1)
C     DRMAX=DR1(MAX)
C
C                      DEFINE ALL DZ'S
C
      DO 100 J=1,N
  100 Z1(J)=(J-1)*200.E2
      DO 110 J=1,N1
  110 DZ1(J)=Z1(J+1)-Z1(J)
      DZ2(1)=2.*(0.5*DZ1(1)-Z1(1))
      Z2(1)=0.5*DZ2(1)
      DO 120 J=2,N1
      DZ2(J)=0.5*(DZ1(J)+DZ1(J-1))
  120 Z2(J)=Z2(J-1)+DZ2(J)
      DZ2(N)=2.*(Z1(N)-Z1(N-1)-0.5*DZ1(N1))
C
C                      A AND B ARE CONSTANT USED IN SUBROUTINE BOUNDV
C                      FOR CONSTANT DIV. AND VORT. CONDITIONS
C
      BNDA=R1(M1)/R1(M)
      BNDB=(R1(M1)+R1(M))*DR1(M1)/((R1(M1)+R1(M2))*R1(M)*DR1(M2))
      BNDB=0.
C
C                      DEFINE DENSITY RELATED CONSTANTS
C
      RHO=1.
      DO 130 J=1,N
  130 BV2(J)=1.E-4
      TBV=0.
      DO 135 J=1,N
  135 TBV=AMAX1(TBV,BV2(J))
      TBV=1./SQRT(TBV)
C
C                      DEFINE HORIZONTAL AND VERTICAL DIFFUSION COEFFIENTS
C
      COEFH=0.002*DR1(1)**2/DELT
      COEFZ=0.001*DZ1(1)**2/DELT
      DO 140 I=1,M1
  140 HK(I)=COEFH*(1.+5.*EXP(-FLOAT(M1-I)/7.))
      DO 150 J=1,N1
  150 ZK(J)=COEFZ*(1.+5.*(EXP(-FLOAT(J-1)/5.)+EXP(-FLOAT(N1-J)/5.)))
      RETURN
      END
```

CARD IMAGE FILE EDITOR(CIFER) -- VERSION 05.29 DATE=10/26/82 TIME=14:16:32:36

*** MEMBER START

```
      SUBROUTINE START
      PARAMETER M=21,N=21
      PARAMETER M1=M-1,M2=M-2,N1=N-1,N2=N-2
      COMMON/ONE/VR1(M,N1),VT1(M,N1),B1(M1,N1),VR2(M,N1),
     1          VT2(M,N1),B2(M1,N1),VR3(M,N1),VT3(M,N1),
     2          B3(M1,N1),P(M1,N1),VZ(M1,N)
      COMMON/TWO/R1(M),R2(M1),DR1(M1),DR2(M),Z1(N),Z2(N1),DZ1(N1),DZ2(N)
      COMMON/THR/RHO,BNOR(N1),BV2(N),ALPHA,BNDA,BNDB,CORI,G,HK(M),ZK(N)
      PARAMETER ND=2*M*N1+M1*N1
      DIMENSION DATA1(ND),DATA2(ND)
      EQUIVALENCE (DATA1,VR1),(DATA2,VR2)
C
C                     INITIALIZE MASS FIELDS FOR A THEORETICAL RING
C
      I11=1
      I12=13
      I21=I12+1
      I22=M1
      BMAG=.0002
      DO 10 I=I11,I12
   10 B1(I,N1)=BMAG*COS(FLOAT(I-I11)/8.*3.14159)*G/RHO
      DO 30 I=I21,I22
   30 B1(I,N1)=B1(I12,N1)*EXP(-FLOAT(I-I21+1)/4.)
      DO 40 J=1,N2
      FACT=EXP(FLOAT(J-N1)/5.)
      DO 40 I=1,M1
   40 B1(I,J)=B1(I,N1)*FACT
C
C                     PRESSURE IS OBTAINED HYDROSTATICALLY FROM BUOYANCY
C
      DO 50 I=1,M1
   50 P(I,1)=-0.5*RHO*DZ2(1)*B1(I,1)
      DO 60 J=2,N1
      DO 60 I=1,M1
   60 P(I,J)=P(I,J-1)-0.5*RHO*DZ2(J)*(B1(I,J)+B1(I,J-1))
C
C                     TANGENTIAL VELOCITY IS AT GRADIENT BALANCE
C
      DO 70 J=1,N1
      DO 70 I=2,M1
      PGF=(P(I,J)-P(I-1,J))/(RHO*DR2(I))
      RAD=(0.5*CORI*R1(I))**2+R1(I)*PGF
      JJ=J
      II=I
      IF(RAD.LT.0.)GO TO 100
   70 VT1(I,J)=-0.5*CORI*R1(I)+SQRT(RAD)
C
C                     SET DATA2=DATA1 FOR LEAPFROG
C
      DO 80 I=1,ND
   80 DATA2(I)=DATA1(I)
      CALL BOUNDV
      DO 90 I=1,ND
   90 DATA1(I)=DATA2(I)
      RETURN
  100 PRINT 110,II,JJ,PGF,RAD
  110 FORMAT(' RADICAL IN SUBROUTINE START IS NEGATIVE AT (I,J)=',2I5,
     1' PGF, RAD =',1P2E12.3)
      STOP
      END
```

CARD IMAGE FILE EDITOR(CIFER) -- VERSION 05.29 DATE=10/26/82 TIME=14:16:32:36

*** MEMBER UP

```
      SUBROUTINE UP
      PARAMETER M=21,N=21
      PARAMETER M1=M-1,M2=M-2,N1=N-1,N2=N-2
      COMMON/ONE/VR1(M,N1),VT1(M,N1),B1(M1,N1),VR2(M,N1),
     1           VT2(M,N1),B2(M1,N1),VR3(M,N1),VT3(M,N1),
     2           B3(M1,N1),P(M1,N1),VZ(M1,N)
      COMMON/TWO/R1(M),R2(M1),DR1(M1),DR2(M),Z1(N),Z2(N1),DZ1(N1),DZ2(N)
      COMMON/THR/RHO,RHER(N1),BV2(N),ALPHA,BNDA,BNDB,CBRI,G,HK(M),ZK(N)
      PARAMETER M1N=M1*N
      DATA VZ/M1N*0./
C
C                      PRESSURE IS OBTAINED HYDROSTATICALLY FROM B
C
      DO 10 I=1,M1
   10 P(I,1)=-0.5*RHO*DZ2(I)*B2(I,1)
      DO 20 J=2,N1
      DO 20 I=1,M1
   20 P(I,J)=P(I,J-1)-0.5*RHO*DZ2(J)*(B2(I,J)+B2(I,J-1))
C
C                      DIAGNOSE VERTICAL VELOCITY BY CONTINUITY EQUATION
C
      DO 30 J=2,N1
      DO 30 I=1,M1
   30 VZ(I,J)=VZ(I,J-1)+DZ1(J)*(R1(I+1)*VR2(I+1,J-1)-R1(I)*VR2(I,J-1))
     1        /(DR1(I)*0.5*(R1(I+1)+R1(I)))
      RETURN
      END
```

```
CARD IMAGE FILE EDITOR(CIFEM) -- VERSION 05.29  DATE=10/26/82       TIME=14:16:32:36

*** MEMBER BOUNDV

      SUBROUTINE BOUNLV
      PARAMETER M=21,N=21
      PARAMETER M1=M-1,M2=M-2,N1=N-1,N2=N-2
      COMMON/ONE/VR1(M,N1),VT1(M,N1),B1(M1,N1),VR2(M,N1),
     1          VT2(M,N1),B2(M1,N1),VR3(M,N1),VT3(M,N1),
     2          B3(M1,N1),P(M1,N1),V2(M1,N)
      COMMON/TWO/R1(M),R2(M1),DR1(M1),DR2(M),Z1(N),Z2(N1),DZ1(N1),DZ2(N)
      COMMON/THR/RHO,RHOR(N1),BV2(N),ALPHA,BNDA,BNDB,CORI,G,HW(M),ZK(N)
C
C                  LATERAL BOUNDARY FOR TANGENTIAL AND RADIAL VELOCITIES
C                  ASSUMING CONTINUOUS VORTICITY AND DIVERGENCE
C
      DO 10 J=1,N1
      VR2(M,J)=BNDA*VR2(M1,J)+BNDB*(R1(M1)*VR2(M1,J)-R1(M2)*VR2(M2,J))
   10 VT2(M,J)=BNDA*VT2(M1,J)+BNDB*(R1(M1)*VT2(M1,J)-R1(M2)*VT2(M2,J))
      RETURN
      END
```

*** MEMBER DIFF

```
      SUBROUTINE DIFF
C
C                     COMPLTE THE DIFFUSION TERMS
C
      PARAMETER M=21,N=21
      PARAMETER M1=M-1,M2=M-2,N1=N-1,N2=N-2
      COMMON/ONE/VR1(M,N1),VT1(M,N1),B1(M1,N1),VR2(M,N1),
     1           VT2(M,N1),B2(M1,N1),VR3(M,N1),VT3(M,N1),
     2           B3(M1,N1),P(M1,N1),VZ(M1,N)
      COMMON/TWO/R1(M),R2(M1),DR1(M1),DR2(M),Z1(N),Z2(N1),DZ1(N1),DZ2(N)
      COMMON/THR/RHO,RHOB(N1),BV2(N),ALPHA,BNDA,BNDB,CORI,G,HK(M),ZK(N)
      DIMENSION VR(M,N1),VT(M,N1),B(M1,N1)
      EQUIVALENCE (VR,VR1),(VT,VT1),(B,B1)
C
C                     HORIZONTAL DIFFUSION OF RADIAL VELOCITY
C
      DO 10 J=1,N1
      DO 10 I=2,M1
   10 VR3(I,J)=VR3(I,J)+HK(I)*(((VR(I+1,J)-VR(I,J))/DR1(I)
     1       -(VR(I,J)-VR(I-1,J))/DR1(I-1))/DR2(I)-VR(I,J)/(R1(I)*R1(I))
     2         +0.5*((VR(I+1,J)-VR(I,J))/(DR1(I)*R2(I))
     3         +(VR(I,J)-VR(I-1,J))/(DR1(I-1)*R2(I-1))))
C
C                     HORIZONTAL DIFFUSION OF TANGENTIAL VELOCITY
C
      DO 20 J=1,N1
      DO 20 I=2,M1
   20 VT3(I,J)=VT3(I,J)+HK(I)*(((VT(I+1,J)-VT(I,J))/DR1(I)
     1       -(VT(I,J)-VT(I-1,J))/DR1(I-1))/DR2(I)-VT(I,J)/(R1(I)*R1(I))
     2         +0.5*((VT(I+1,J)-VT(I,J))/(DR1(I)*R2(I))
     3         +(VT(I,J)-VT(I-1,J))/(DR1(I-1)*R2(I-1))))
C
C                     HORIZONTAL DIFFUSION OF B
C
      DO 60 J=1,N1
      DO 60 I=2,M2
   60 B3(I,J)=B3(I,J)+HK(I)*(((B(I+1,J)-B(I,J))/DR2(I+1)
     1         -(B(I,J)-B(I-1,J))/DR2(I))/DR1(I)
     2         +0.5*((B(I+1,J)-B(I,J))/(DR2(I+1)*R1(I+1))
     3         +(B(I,J)-B(I-1,J))/(DR2(I)*R1(I))))
      DO 70 J=1,N1
   70 B3(1,J)=B3(1,J)+HK(1)*((B(2,J)-B(1,J))/(DR2(2)*DR1(1))
     1         +0.5*(B(2,J)-B(1,J))/(DR2(2)*R1(2)))
      DO 80 J=1,N1
   80 B3(M1,J)=B3(M1,J)+HK(M1)*((-B(M1,J)+B(M2,J))/(DR2(M1)*DR1(M1))
     1         -(B(M1,J)-B(M2,J))/(DR2(M1)*R1(M1)))
C
C                     VERTICAL DIFFUSION OF RADIAL VELOCITY
C
      DO 90 J=2,N2
      DO 90 I=2,M1
   90 VR3(I,J)=VR3(I,J)+ZK(J)*((VR(I,J+1)-VR(I,J))/DZ2(J+1)
     1         -(VR(I,J)-VR(I,J-1))/DZ2(J))/DZ1(J)
      DO 100 I=2,M1
  100 VR3(I,1)=VR3(I,1)+ZK(1)*(VR(I,2)-VR(I,1))/(DZ2(2)*DZ1(1))
      DO 110 I=2,M1
  110 VR3(I,N1)=VR3(I,N1)+ZK(N1)*(-VR(I,N1)+VR(I,N2))/(DZ2(N1)*DZ1(N1))
C
C                     VERTICAL DIFFUSION OF TANGENTIAL VELOCITY
C
      DO 120 J=2,N2
      DO 120 I=2,M1
  120 VT3(I,J)=VT3(I,J)+ZK(J)*((VT(I,J+1)-VT(I,J))/DZ2(J+1)
     1         -(VT(I,J)-VT(I,J-1))/DZ2(J))/DZ1(J)
      DO 130 I=2,M1
  130 VT3(I,1)=VT3(I,1)+ZK(1)*(VT(I,2)-VT(I,1))/(DZ2(2)*DZ1(1))
      DO 140 I=2,M1
  140 VT3(I,N1)=VT3(I,N1)+ZK(N1)*(-VT(I,N1)+VT(I,N2))/(DZ2(N1)*DZ1(N1))
```

*** MEMBER DIFF

```
C
C                         VERTICAL DIFFUSION OF B
C
      DO 160 J=2,N2
      DO 160 I=1,M1
  160 B3(I,J)=B3(I,J)+ZK(J)*((B1(I,J+1)-B(I,J))/DZ2(J+1)
     1             -(B(I,J)-B(I,J-1))/DZ2(J))/DZ1(J)
      DO 170 I=1,M1
  170 B3(I,1)=B3(I,1)+ZK(1)*(B(I,2)-B(I,1))/(DZ2(2)*DZ1(1))
      DO 180 I=1,M1
  180 B3(I,N1)=B3(I,N1)+ZK(N1)*(-B(I,N1)+B(I,N2))/(DZ2(N1)*DZ1(N1))
      RETURN
      END
```

CARD IMAGE FILE EDITOR(CIFEM) -- VERSION 05.29 DATE=10/26/82 TIME=14:16:32:36

*** MEMBER FRWRD

```
      SUBROUTINE FRWRD
      PARAMETER M=21,N=21
      PARAMETER M1=M-1,M2=M-2,N1=N-1,N2=N-2
      PARAMETER ND=2*M*N1+M1*N1
      COMMON/ONE/DATA1(ND),DATA2(ND),DATA3(ND),P(M1,N1),V2(M1,N)
      COMMON/THR/RHO,RHOR(N1),BV2(N),ALPHA,BNDA,BNDB,CORI,G,HX(M),ZK(N)
      COMMON/FOR/DELT,XTIME,ITIME,ISTEP,ISMO,ITAPE,TBV
C
C                    REPLACE DATA3 WITH THE NEW VALUES
C
      DO 10 I=1,ND
   10 DATA3(I)=DATA1(I)+2.*DELT*DATA3(I)
C
C                    TIME SMOOTHING
C
      IF(MOD(ISTEP,ISMO).NE.0)GO TO 30
      DO 20 I=1,ND
   20 DATA2(I)=DATA2(I)+(DATA1(I)+DATA3(I)-2.*DATA2(I))*ALPHA
   30 CONTINUE
C
C                    FORWARD MARCHING
C
      DO 40 I=1,ND
   40 DATA1(I)=DATA2(I)
      DO 50 I=1,ND
   50 DATA2(I)=DATA3(I)
C
C                     ZERO OUT DATA3 FOR NEXT STEP
C
      DO 60 I=1,ND
   60 DATA3(I)=0.
      RETURN
      END
```

CARD IMAGE FILE EDITOR(CIFEM) -- VERSION 05.29 DATE=10/26/82   TIME=14:16:32:36

*** MEMBER CHECK

```
      SUBROUTINE CHECK
      PARAMETER M=21,N=21
      PARAMETER M1=M-1,M2=M-2,N1=N-1,N2=N-2
      COMMON/ONE/VR1(M,N1),VT1(M,N1),B1(M1,N1),VR2(M,N1),
     1           VT2(M,N1),B2(M1,N1),VR3(M,N1),VT3(M,N1),
     2           B3(M1,N1),P(M1,N1),VZ(M1,N)
      COMMON/TWO/R1(M),R2(M1),DR1(M1),DR2(M),Z1(N),Z2(N1),DZ1(N1),DZ2(N)
      COMMON/FOR/DELT,XTIME,ITIME,ISTEP,ISMP,ITAPE,TBV
      DIMENSION WORK1(M),WORK2(N)
      DO 10 J=1,N1
      DO 20 I=1,M
   20 WORK1(I)=DR2(I)/AMAX1(1.,VR2(I,J))
      MIN=MINMAG(WORK1)+1
      DT=WORK1(MIN)*0.9
      DT=AMIN1(DT,DELT)
   10 CONTINUE
      DT=AMIN1(DT,TBV)
      IF(DT.GE.DELT)RETURN
      DELT=0.75*DELT
      PRINT 100,DELT
  100 FORMAT(//////,'********DELT IS CHANGED TO',1PE11.2,' SMALLER***')
      RETURN
      END
```

CARD IMAGE FILE EDITOR(CIFEM) -- VERSION 05.29 DATE=10/26/82 TIME=14:16:32:36

*** MEMBER ADVECT

```
      SUBROUTINE ADVECT
C
C                    COMPLTE THE ADVECTIVE TERMS
C
      PARAMETER M=21,N=21
      PARAMETER M1=M-1,M2=M-2,N1=N-1,N2=N-2
      COMMON/ONE/VR1(M,N1),VT1(M,N1),B1(M1,N1),VR2(M,N1),
     1           VT2(M,N1),B2(M1,N1),VR3(M,N1),VT3(M,N1),
     2           B3(M1,N1),P(M1,N1),VZ(M1,N)
      COMMON/TWO/R1(M),R2(M1),DR1(M1),DR2(M),Z1(N),Z2(N1),DZ1(N1),DZ2(N)
      COMMON/THR/RHO,RHOR(N1),BV2(N),ALPHA,BNDA,BNDB,CORI,G,HK(M),ZK(N)
      DIMENSION VR(M,N1),VT(M,N1),B(M1,N1)
      EQUIVALENCE (VR,VR2),(VT,VT2),(B,B2)
C
C                    HORIZONTAL ADVECTION FOR RADIAL VELOCITY
C
      DO 10 J=1,N1
      DO 10 I=2,M1
   10 VR3(I,J)=-0.25*((VR(I,J)+VR(I-1,J))*(VR(I,J)-VR(I-1,J))/DR1(I-1)
     1           +(VR(I+1,J)+VR(I,J))*(VR(I+1,J)-VR(I,J))/DR1(I))
     2           +VR3(I,J)
C
C                    HORIZONTAL ADVECTION FOR TANGENTIAL VELOCITY
C
      DO 20 J=1,N1
      DO 20 I=2,M1
   20 VT3(I,J)=-0.25*((VR(I,J)+VR(I-1,J))*(VT(I,J)-VT(I-1,J))/DR1(I-1)
     1           +(VR(I+1,J)+VR(I,J))*(VT(I+1,J)-VT(I,J))/DR1(I))
     2           +VT3(I,J)
C                    HORIZONTAL ADVECTION FOR BUOYANCY
C
      DO 60 J=1,N1
      DO 60 I=2,M2
   60 B3(I,J)=B3(I,J)-0.5*(VR(I,J)*(B(I,J)-B(I-1,J))/DR2(I)
     1           +VR(I+1,J)*(B(I+1,J)-B(I,J))/DR2(I+1))
      DO 70 J=1,N1
   70 B3(1,J)=B3(1,J)-0.5*VR(2,J)*(B(2,J)-B(1,J))/DR2(2)
      DO 80 J=1,N1
   80 B3(M1,J)=B3(M1,J)-0.5*VR(M1,J)*(B(M1,J)-B(M2,J))/DR2(M1)
C
C                    VERTICAL ADVECTION FOR RADIAL VELOCITY
C
      DO 90 J=2,N2
      DO 90 I=2,M1
   90 VR3(I,J)=VR3(I,J)-0.25*((VZ(I-1,J)+VZ(I,J))*(VR(I,J)-VR(I,J-1))
     1          /DZ2(J)+(VZ(I,J+1)+VZ(I-1,J+1))*(VR(I,J+1)-VR(I,J))
     2          /DZ2(J+1))
      DO 95 I=2,M1
   95 VR3(I,1)=VR3(I,1)-0.25*(VZ(I,2)+VZ(I-1,2))*(VR(I,2)-VR(I,1))
     1          /DZ2(2)
      DO 96 I=2,M1
   96 VR3(I,N1)=VR3(I,N1)-0.25*(VZ(I-1,N1)+VZ(I,N1))*(VR(I,N1)-VR(I,N2))
     1          /DZ2(N1)
C
C                    VERTICAL ADVECTION FOR TANGENTIAL VELOCITY
C
      DO 100 J=2,N2
      DO 100 I=2,M1
  100 VT3(I,J)=VT3(I,J)-0.25*((VZ(I-1,J)+VZ(I,J))*(VT(I,J)-VT(I,J-1))
     1          /DZ2(J)+(VZ(I,J+1)+VZ(I-1,J+1))*(VT(I,J+1)-VT(I,J))
     2          /DZ2(J+1))
      DO 105 I=2,M1
  105 VT3(I,1)=VT3(I,1)-0.25*(VZ(I,2)+VZ(I-1,2))*(VT(I,2)-VT(I,1))
     1          /DZ2(2)
      DO 106 I=2,M1
  106 VT3(I,N1)=VT3(I,N1)-0.25*(VZ(I,N1)+VZ(I-1,N1))*(VT(I,N1)-VT(I,N2))
     1          /DZ2(N1)
C
C                    VERTICAL ADVECTION FOR B
C
      DO 150 J=2,N2
      DO 150 I=1,M1
  150 B3(I,J)=B3(I,J)-0.5*(VZ(I,J)*(B(I,J)-B(I,J-1))/DZ2(J)
     1          +VZ(I,J+1)*(B(I,J+1)-B(I,J))/DZ2(J+1))
      DO 160 I=1,M1
  160 B3(I,1)=B3(I,1)-0.5*VZ(I,2)*(B2(I,2)-B2(I,1))/DZ2(2)
      DO 170 I=1,M1
```

*** MEMBER ADVECT

```
  170 B3(I,N1)=B3(I,N1)-0.5*VZ(I,N1)*(B(I,N1)-B(I,N2))/DZ2(N1)
C
C                       INERTIA TERMS FOR HORIZONTAL MOMENTUM
C
      DO 110 J=1,N1
      DO 110 I=2,M1
      VR3(I,J)=VR3(I,J)+VT(I,J)*(VT(I,J)/R1(I)+CORI)
  110 VT3(I,J)=VT3(I,J)-VR(I,J)*(VT(I,J)/R1(I)+CORI)
C
C                       PRESSURE GRADIENT FORCE
C
      DO 120 J=1,N1
      DO 120 I=2,M1
  120 VR3(I,J)=VR3(I,J)-(P(I,J)-P(I-1,J))/(RHO*DR2(I))
C
C                       STRATIFICATION TERM
C
      DO 130 J=1,N1
      DO 130 I=1,M1
  130 B3(I,J)=B3(I,J)+0.5*(VZ(I,J)*BV2(J)+VZ(I,J+1)*BV2(J+1))
      RETURN
      END
```

*** MEMBER PUTOUT

```
      SUBROUTINE PUTOUT
      PARAMETER M=21,N=21
      PARAMETER M1=M-1,M2=M-2,N1=N-1,N2=N-2
      COMMON/ONE/VR1(M,N1),VT1(M,N1),B1(M1,N1),VR2(M,N1),
     1           VT2(M,N1),B2(M1,N1),VR3(M,N1),VT3(M,N1),
     2           B3(M1,N1),P(M1,N1),VZ(M1,N)
      COMMON/TWO/R1(M),R2(M1),DR1(M1),DR2(M),Z1(N),Z2(N1),DZ1(N1),DZ2(N)
      COMMON/THR/RHO,RHOR(N1),BV2(N),ALPHA,BNDA,BNDB,CORI,G,HK(M),ZK(N)
      COMMON/FOR/DELT,XTIME,ITIME,ISTEP,ISMO,ITAPE,TBV
C
C                   THIS SUBROUTINE PRINT OUT FIELDS FOR A QUICK LOOK
C
      DIMENSION IDUM(M,N)
  700 FORMAT(////,'  RADIAL VELOCITY (CM/S) AT T=',I6,' M')
  705 FORMAT(////,'  TANGENTIAL VELOCITY (CM/S) AT T=',I6,' M')
  710 FORMAT(////,'  VERTICAL VELOCITY (CM/S) AT T=',I6,' M')
  715 FORMAT(////,'  BUOYANCY FIELD (*.001) AT T=',I6,' M')
  725 FORMAT(////,'  PRESSURE (*10 DYNE/CM**2) AT TIME=',I6,' M')
  720 FORMAT(1H1,////,20X,'**********    OUTPUT AT TIME =',I6,' M    OR',
     1 F8.2,' DAY      ISTEP =',I7,'    *************')
      DAY=XTIME/86400.+0.0001
      PRINT 720,ITIME,DAY,ISTEP
      DO 10 J=1,N1
      DO 10 I=1,M
   10 IDUM(I,J)=VR2(I,J)
      PRINT 700,ITIME
      CALL MAP(IDUM,R1,Z2,M,N1)
      DO 20 J=1,N1
      DO 20 I=1,M
   20 IDUM(I,J)=VT2(I,J)
      PRINT 705,ITIME
      CALL MAP(IDUM,R1,Z2,M,N1)
      DO 30 J=1,N
      DO 30 I=1,M1
   30 IDUM(I,J)=VZ(I,J)
      PRINT 710,ITIME
      CALL MAP(IDUM,R2,Z1,M1,N)
      DO 40 J=1,N1
      DO 40 I=1,M1
   40 IDUM(I,J)=B2(I,J)*1.E3
      PRINT 715,ITIME
      CALL MAP(IDUM,R2,Z2,M1,N1)
      DO 50 J=1,N1
      DO 50 I=1,M1
   50 IDUM(I,J)=P(I,J)*1.E-1
      PRINT 725,ITIME
      CALL MAP(IDUM,R2,Z2,M1,N1)
      RETURN
      END
```

```
CARD IMAGE FILE EDITOR(CIFED) -- VERSION 05.29  DATE=10/26/82        TIME=14:11:32:36

*** MEMBER MAP

      SUBROUTINE MAP(A,R,Z,MM,NN)
      PARAMETER M=21,N=21
      DIMENSION R(MM),Z(NN)
      INTEGER A (M,N),IR(M),IZ(N)
   70 FORMAT(1H5,7X,25I5)
   80 FORMAT(1H5,I4,3X,25I5)
      MP=MIN0(25,MM)
      DO 10 I=1,MP
   10 IR(I)=R(I)*1.E-5+0.1
      DO 20 J=1,NN
   20 IZ(J)=Z(J)*1.E-2+0.1
      PRINT 70
      PRINT 70,(IR(I),I=1,MP)
      PRINT 70
      DO 30 JJ=1,NN
      J=NN+1-JJ
   30 PRINT 80,IZ(J),(A(I,J),I=1,MP)
      RETURN
      END
```

END

FILMED

02-84

DTIC